



HAL
open science

Gene Coexpression Analysis Reveals Complex Metabolism of the Monoterpene Alcohol Linalool in Arabidopsis Flowers

Jean-François Ginglinger, Benoit Boachon, René Höfer, Christian Paetz, Tobias G Köllner, Laurence Miesch, Raphael Lugan, Raymonde Baltenweck, Jérôme Mutterer, Pascaline Ullmann, et al.

► **To cite this version:**

Jean-François Ginglinger, Benoit Boachon, René Höfer, Christian Paetz, Tobias G Köllner, et al.. Gene Coexpression Analysis Reveals Complex Metabolism of the Monoterpene Alcohol Linalool in Arabidopsis Flowers. *The Plant cell*, 2013, 25, pp.4640 - 4657. 10.1105/tpc.113.117382 . hal-04652352

HAL Id: hal-04652352

<https://hal.science/hal-04652352v1>

Submitted on 18 Jul 2024

HAL is a multi-disciplinary open access archive for the deposit and dissemination of scientific research documents, whether they are published or not. The documents may come from teaching and research institutions in France or abroad, or from public or private research centers.

L'archive ouverte pluridisciplinaire **HAL**, est destinée au dépôt et à la diffusion de documents scientifiques de niveau recherche, publiés ou non, émanant des établissements d'enseignement et de recherche français ou étrangers, des laboratoires publics ou privés.

Gene Coexpression Analysis Reveals Complex Metabolism of the Monoterpene Alcohol Linalool in *Arabidopsis* Flowers ^{WJOPEN}

Jean-François Ginglinger,^a Benoit Boachon,^a René Höfer,^{a,1} Christian Paetz,^b Tobias G. Köllner,^b Laurence Miesch,^c Raphael Lukan,^a Raymonde Baltenweck,^d Jérôme Mutterer,^a Pascaline Ullmann,^a Franziska Beran,^b Patricia Claudel,^d Francel Verstappen,^e Marc J.C. Fischer,^d Francis Karst,^d Harro Bouwmeester,^e Michel Miesch,^c Bernd Schneider,^b Jonathan Gershenzon,^b Jürgen Ehling,^f and Danièle Werck-Reichhart^{a,2}

^aInstitute of Plant Molecular Biology, Centre National de la Recherche Scientifique Unité Propre de Recherche 2357, University of Strasbourg, F-67000 Strasbourg, France

^bMax Planck Institute for Chemical Ecology, D-07745 Jena, Germany

^cLaboratoire de Chimie Organique Synthétique, Centre National de la Recherche Scientifique Unité Mixte de Recherche 7177, University of Strasbourg, France

^dLaboratoire Métabolisme Secondaire de la Vigne, Institut National de la Recherche Agronomique Unité Mixte de Recherche 1131, University of Strasbourg, Colmar, F-68021 France

^eLaboratory of Plant Physiology, Wageningen University, 6700 AR Wageningen, The Netherlands

^fDepartment of Biology, Centre for Forest Biology, University of Victoria, Victoria, British Columbia V8P 5C2, Canada

The cytochrome P450 family encompasses the largest family of enzymes in plant metabolism, and the functions of many of its members in *Arabidopsis thaliana* are still unknown. Gene coexpression analysis pointed to two P450s that were coexpressed with two monoterpene synthases in flowers and were thus predicted to be involved in monoterpene metabolism. We show that all four selected genes, the two terpene synthases (*TPS10* and *TPS14*) and the two cytochrome P450s (*CYP71B31* and *CYP76C3*), are simultaneously expressed at anthesis, mainly in upper anther filaments and in petals. Upon transient expression in *Nicotiana benthamiana*, the TPS enzymes colocalize in vesicular structures associated with the plastid surface, whereas the P450 proteins were detected in the endoplasmic reticulum. Whether they were expressed in *Saccharomyces cerevisiae* or in *N. benthamiana*, the TPS enzymes formed two different enantiomers of linalool: (–)-(R)-linalool for *TPS10* and (+)-(S)-linalool for *TPS14*. Both P450 enzymes metabolize the two linalool enantiomers to form different but overlapping sets of hydroxylated or epoxidized products. These oxygenated products are not emitted into the floral headspace, but accumulate in floral tissues as further converted or conjugated metabolites. This work reveals complex linalool metabolism in *Arabidopsis* flowers, the ecological role of which remains to be determined.

INTRODUCTION

A prolific expansion of the cytochrome P450 (*CYP*) gene family in land plants has generated the largest family of enzymes in plant metabolism (Nelson and Werck-Reichhart, 2011). Because P450s usually catalyze specific slow and rate-limiting steps in metabolic pathways, the complexity of the P450 superfamily is expected to reflect the complexity of plant metabolism. Despite rapid advances in recent years (Bak et al., 2011; Hamberger and Bak, 2013), the function of a large proportion of the plant P450 enzymes remains either unknown or only superficially understood. The main objective of our work is to determine the function of new P450 families

and subgroups using *Arabidopsis thaliana* as a model. To obtain leads to the function of as-yet-uncharacterized P450 enzymes, a predictive strategy based on gene coexpression analysis was recently implemented (Ehling et al., 2008; <http://www-ibmp.u-strasbg.fr/~CYPedia/>), which led to the identification of orphan P450 functions in lipid, phenolic, and hormone metabolism (Matsuno et al., 2009; Sauveplane et al., 2009; Heitz et al., 2012). This predictive strategy also pointed to several sets of coexpressed genes predicted to be involved in terpenoid metabolism (Ehling et al., 2008). Two of these gene sets were confirmed to be involved in the metabolism of the triterpenes thalianol (Field and Osbourn, 2008) and marneral (Field et al., 2011). Several other sets provide leads for sesquiterpenoid and monoterpene metabolism and other pathways of triterpene metabolism.

Arabidopsis had long been considered devoid of volatile terpenoids until genome sequencing revealed the presence of a quite large set of monoterpene and sesquiterpene synthases (Aubourg et al., 2002). A complex bouquet of volatile compounds, including more than 24 monoterpenes and 26 sesquiterpenes, was found emitted from inflorescences and other aerial parts of the plant (Aharoni et al., 2003; Chen et al., 2003; Steeghs

¹ Current address: VIB Department of Plant Systems Biology, Ghent University Technologiepark 927, 9052 Gent, Belgium.

² Address correspondence to daniele.werck@ibmp-cnrs.unistra.fr.

The author responsible for distribution of materials integral to the findings presented in this article in accordance with the policy described in the Instructions for Authors (www.plantcell.org) is: Danièle Werck-Reichhart (daniele.werck@ibmp-cnrs.unistra.fr).

^{WJOPEN} Online version contains Web-only data.

^{OPEN} Articles can be viewed online without a subscription.

www.plantcell.org/cgi/doi/10.1105/tpc.113.117382

et al., 2004; Rohloff and Bones, 2005). It also comprised several oxygenated compounds such as the lilac aldehydes, α -terpineol, verbenone, and longiborneol. 1,8-Cineole was the main terpenoid found to be emitted from roots (Steeghs et al., 2004).

Most monoterpene and sesquiterpene synthases from *Arabidopsis* have now been characterized. The first was terpene synthase 10 (TPS10), which is highly expressed in flowers. When expressed in *Escherichia coli*, TPS10 was found to have mainly β -myrcene and (*E*)- β -ocimene synthase activity (Bohlmann et al., 2000). Three other genes expressed almost exclusively in flowers were shown to encode enzymes producing (+)-(3*S*)-linalool (TPS14), (–)-(*E*)- β -caryophyllene and α -humulene (TPS21), α -pinene, β -pinene, β -myrcene, limonene, and (*E*)- β -ocimene (TPS24) as main products (Chen et al., 2003). (*E*)- β -Ocimene and (*E,E*)- α -farnesene were produced in vitro by two enzymes encoded by other flower-expressed tandem duplicated paralogs: TPS3 (functional in the ecotype *Col-0*) and TPS2 (functional in Wassilewskija) (Fäldt et al., 2003; Huang et al., 2010). The respective in vivo activities of the latter, however, appeared modulated by its different subcellular localization (Huang et al., 2010). Most of the floral sesquiterpene emission was found to rely on only two TPSs (TPS21 and TPS11), producing a complex blend with (–)-(*E*)- β -caryophyllene (TPS21), (+)-thujopsene, and (+)- β -chamigrene (TPS11) as main products (Tholl et al., 2005). The other TPSs characterized thus far are predominantly expressed in roots, and include products of two tandem duplicated genes, TPS23 and TPS27, which both form a blend of monoterpenes with 1,8-cineole as major products (Chen et al., 2003). TPS12 and TPS13 were shown to form a blend of sesquiterpenes with (*Z*)- γ -bisabolene being the major product (Ro et al., 2006). Not all TPS products are detectable in the volatile fraction of plant metabolites. This suggests that instead of being emitted as volatiles, they may be further converted into more hydrophilic (e.g., oxygenated and possibly further modified or conjugated) compounds retained in plant tissues. Oxidative monoterpene and sesquiterpene metabolism is expected to involve P450 enzymes, and several examples of TPS and P450 coexpression can be found in databases (Ehltling et al., 2008; Tholl and Lee, 2011). In addition, several cases of physical associations of monoterpene and sesquiterpene synthases with P450 genes can be found in the *Arabidopsis* genome, which suggest that this clustering is not fortuitous and may correspond to functional units (Tholl and Lee, 2011). However, no monoterpene- or sesquiterpene-metabolizing cytochrome P450 in *Arabidopsis* has been reported thus far. The only described P450 enzyme to be involved in the biosynthesis of a volatile terpenoid compound is CYP82G1, which is responsible for the breakdown of the C20-precursor (*E,E*)-geranylinalool into the C16 homoterpene (*E,E*)-4,8,12-trimethyltrideca-1,3,7,11-tetraene and of the C15 (*E*)-nerolidol into the C11-homoterpene (*E*)-4,8-dimethyl-1,3,7-nonatriene. Both compounds are common constituents of floral and herbivore-induced plant volatile bouquets (Lee et al., 2010).

We focus here on a set of four genes with strongly correlated floral expression that are predicted to be involved in monoterpene metabolism. This set includes two genes encoding TPSs previously described as a β -myrcene and (*E*)- β -ocimene synthase (TPS10) (Bohlmann et al., 2000) and as a (+)-(3*S*)-linalool synthase

(TPS14) (Chen et al., 2003). The two others, *CYP76C3* and *CYP71B31*, encode P450 enzymes of unknown function. We confirm their tight coexpression and show that it is at its highest during anthesis in the stamen filaments. By recombinant expression in yeast (*Saccharomyces cerevisiae*) and in planta we demonstrate that all four genes contribute to a thus far overlooked and complex linalool metabolism occurring in the flowers of *Arabidopsis*. The role of this metabolism in plant–insect interactions and flower protection against parasite attack requires further investigation.

RESULTS

Coexpression Analysis Identifies Candidate P450 Genes Predicted to be Involved in Monoterpene Metabolism

The coexpression CYPedia tool based on Affymetrix ATH1 microarray data (Ehltling et al., 2008; <http://www-ibmp.u-strasbg.fr/~CYPedia/>) was used to predict potential P450s involved in the metabolism of monoterpenes in *Arabidopsis*. All seven genes described by Aubourg et al. (2002) to encode monoterpene synthases were used as baits to retrieve coexpressed P450s (Figure 1). TPS23 and TPS27 share the same probe set and are coexpressed with 11 P450s with main expression in seedlings and roots. TPS2, TPS3, TPS10, TPS14, and TPS24 are all mainly expressed in flowers and extracted nine P450s. The strongest coregulation was obtained in a group of two monoterpene synthases (TPS10 and TPS14) and two P450s (*CYP76C3* and *CYP71B31*) with correlation coefficients above 0.8 linking them (Figure 1; see Supplemental Figure 1 online). When expressed in *Escherichia coli*, TPS10 (At2g24210) catalyzes the formation of five olefin monoterpenes with β -myrcene and (*E*)- β -ocimene as the main products (Bohlmann et al., 2000). By contrast, TPS14 (At1g61680) catalyzes the stereospecific formation of (+)-(*S*)-linalool (Chen et al., 2003). The coexpressed *CYP76C3* and *CYP71B31* are members of the CYP76 and CYP71 families of P450, respectively; and both families belong to the CYP71 clan. P450s in general and CYP71 family members in particular comprise several examples of monoterpene hydroxylases and epoxidases (Karp et al., 1990; Hallahan et al., 1992, 1994; Lupien et al., 1999; Haudenschield et al., 2000; Berteau et al., 2001; Collu et al., 2001; Aharoni et al., 2004), and as such, constitute excellent candidates for monoterpene oxidation. TPS10, TPS14, *CYP71B31*, and *CYP76C3* were thus chosen for functional investigations.

Candidate TPS and P450 Genes Are Expressed during Anthesis in Petals and Stamen Filaments

Candidate gene expression was next re-evaluated by relative quantitative RT-PCR (qRT-PCR). The levels of TPS10, TPS14, *CYP76C3*, and *CYP71B31* transcripts confirmed their coexpression in the flower (Figure 2). Samples collected from different flower development stages showed a very similar pattern of expression, which was highest at anthesis.

To obtain more precise expression patterns, plant lines transformed with gene promoter: β -glucuronidase (*GUS*) fusion

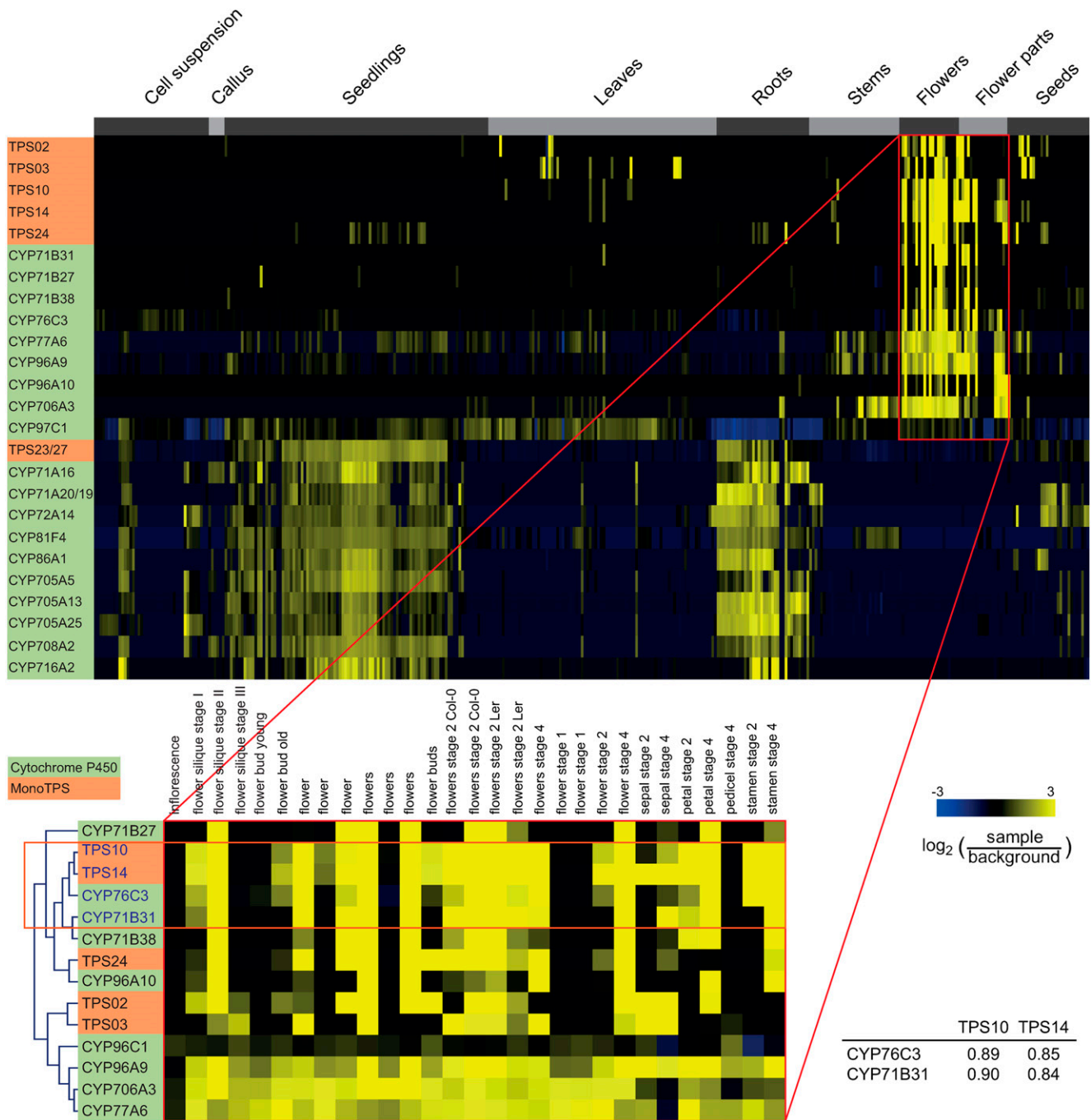


Figure 1. Expression Heatmap of *Arabidopsis* P450s Coexpressed With Monoterpene Synthases in Various Organs and Tissues.

An enlargement of the data for floral organs is shown. Values are based on background corrected Affymetrix microarray data. Color intensity in yellow (positive) or blue (negative) is proportional to \log_2 ratio compared with the mean intensity of all organs and tissues. Genes are clustered according to their coexpression. An expression heatmap with detailed experiment annotation is available in Supplemental Figure 1 online.

constructs were generated for all four candidates. GUS staining of the transformants confirmed the expression of all four genes in the stamen, and more specifically in the upper part of the filament of the open flowers (Figure 3). GUS expression in the petals was also observed for all four genes, but only after extended staining.

The *TPS* promoters were also active in the receptacle near the junction with the style where no GUS staining was observed for both P450s. Conversely, strong staining was observed for the *CYP71B31* and *CYP76C3* promoters in the nectaries, where no expression of the two *TPS*s was detected.

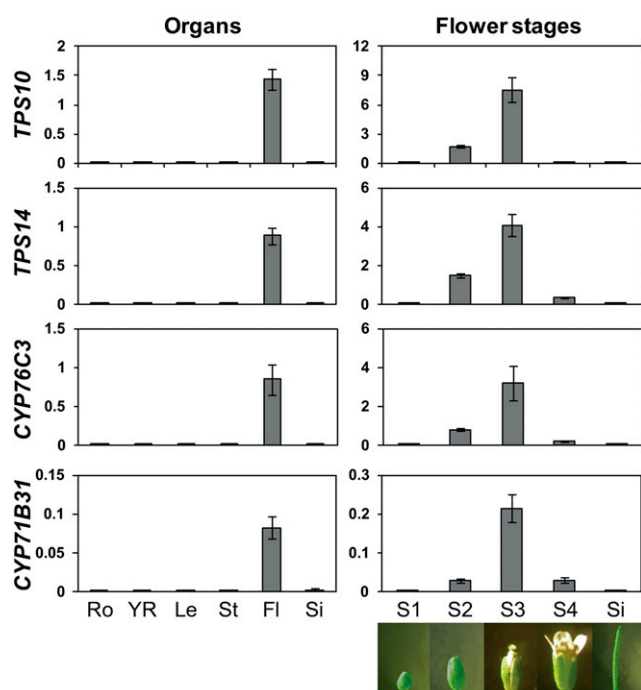


Figure 2. Relative Transcript Levels of Candidate Coexpressed Monoterpene Synthase and P450 Genes in Organs of *Arabidopsis* and at Different Stages of Floral Development.

Transcripts levels were determined by qRT-PCR. The Ct values obtained for the CYP and TPS genes were normalized to the Ct values obtained for four reference genes whose stable expression in *Arabidopsis* tissues is known (Czechowski et al., 2005) and relative expression was calculated with the specific efficiency of each primer pair by using the $E_{\Delta Ct}$ method. Results represent the mean \pm SE of two technical repetitions and five biological replicates for organs, three for flower stages, and four for flower parts. Flower stages are divided into young bud (S1), ready-to-open bud (S2), just-opened bud (S3), fully-open flower (S4), and siliques (S5) as shown. FI, flower; Le, leaf; Ro, root; Si, silique; St, stem; YR, young root.

Subcellular Localization of the Candidate Genes

Tight coexpression of the four selected genes suggested a functional cooperation that would be favored by subcellular colocalization and direct interaction to channel metabolic intermediates. Whereas monoterpene synthases are usually found localized in the plastids (Aharoni et al., 2004; Lee and Chappell, 2008; Nagegowda et al., 2008; Huang et al., 2010), P450s are most often anchored in the endoplasmic reticulum (ER) membranes via an N-terminal 25 to 30 amino acid signal sequence. However, some P450s have been found to be targeted to the plastidial membranes via a longer and more hydrophilic transit peptide (Froehlich et al., 2001; Helliwell et al., 2001; Watson et al., 2001; Tian et al., 2004; Kim and DellaPenna, 2006). The protein sequence of CYP71B31 shows typical characteristics of ER-anchored proteins and is predicted to be localized in the ER by TargetP and Predotar (Emanuelsson et al., 2000; Small et al., 2004). CYP76C3, however, has a longer and more hydrophilic sequence with a significant proportion of Ser and Thr residues, and was previously

suggested to be a plastid-targeted protein (Schuler et al., 2006). Whereas TargetP and Predotar predict the protein to be targeted to the ER with a high probability, ChloroP (Emanuelsson et al., 1999) detects the presence of a potential chloroplast transit peptide at the N terminus of CYP76C3.

To experimentally determine the subcellular localization of the TPS and P450 proteins and their potential for interaction, enhanced green fluorescent protein (eGFP) and monomeric red fluorescent protein (mRFP) fusions were constructed for all four, and transiently expressed via *Agrobacterium tumefaciens*-mediated transfection of *Nicotiana benthamiana* leaves. Confocal microscopy of leaf epidermal cells confirmed that both TPS14 and TPS10 are associated with the chloroplasts (Figures 4A and 4B). However, the proteins seemed compartmented in 5 to 20 globular vesicles of heterogeneous size (up to 1 μ m in diameter) that appear to be associated with the plastid envelope. TPS10 and TPS14 are colocalized in the same vesicles when simultaneously expressed in the same leaf (Figures 4E to 4G). These vesicles do not correspond to the description of any plastidial substructures reported thus far. CYP76C3 and CYP71B31 also showed identical subcellular localizations, and were found exclusively associated with the ER (Figures 4C and 4D; see Supplemental Figure 2 online) in *N. benthamiana*. It is noteworthy, however, that the ER membranes encircle the plastids forming direct contacts with the

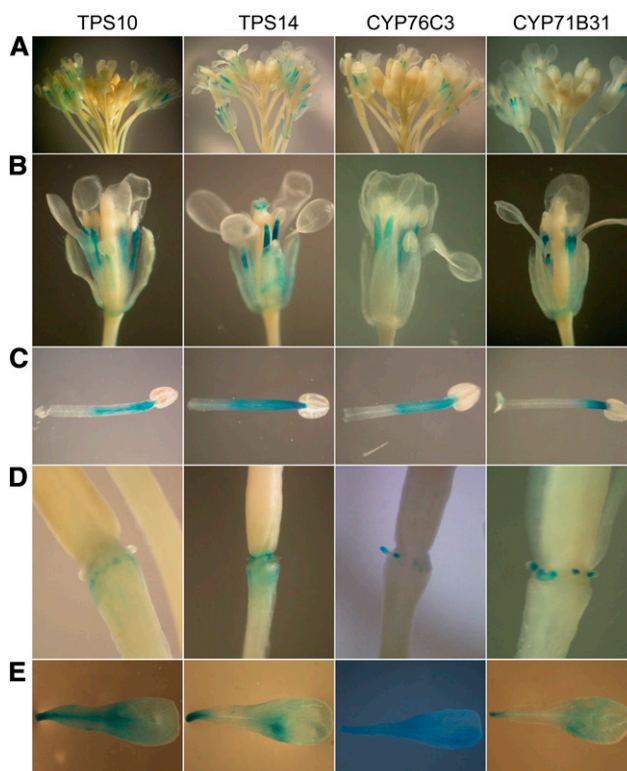


Figure 3. GUS Staining Showing Spatiotemporal Floral Expression of the Candidate Coexpressed *MONOTERPENE SYNTHASE* (TPS) and *P450* (CYP) Genes in *Arabidopsis* Floral Organs.

GUS staining was 4 h for inflorescences (A), fully opened flowers (B), stamens (C), and nectaries (D), and 24 h for petals (E).

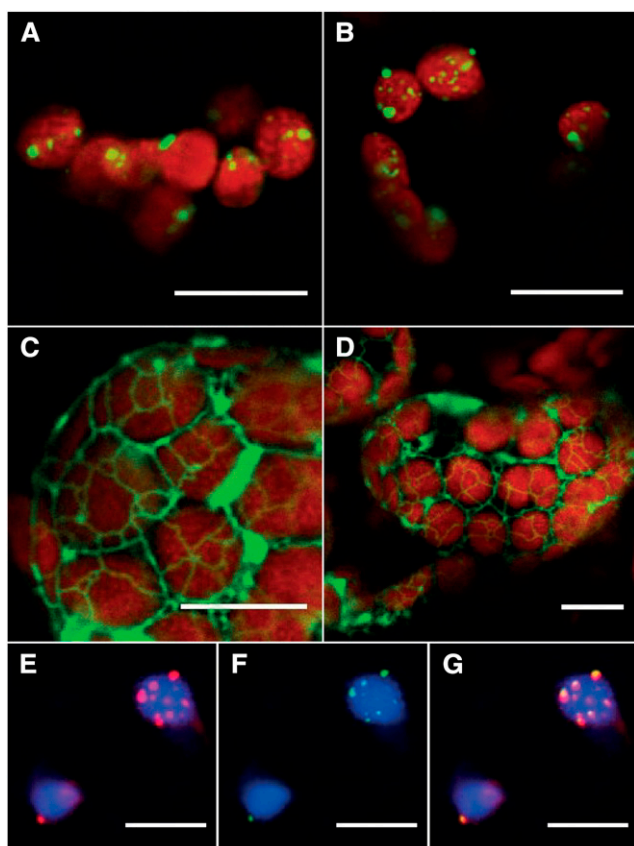


Figure 4. Confocal Fluorescence Microscopy of *N. benthamiana* Epidermal Cells Expressing or Coexpressing eGFP or mRFP-Fused Candidate Proteins.

(A) to (D) Leaves infiltrated with a single construct, merged eGFP, and chlorophyll fluorescence are shown as follows: TPS10:eGFP (A), TPS14:eGFP (B), CYP76C3:eGFP (C), and CYP71B31:eGFP (D).

(E) to (G) Leaves coinfiltrated with TPS10:mRFP and TPS14:eGFP are shown as follows: merged image of TPS10:mRFP and chlorophyll fluorescence (E), TPS14:eGFP and chlorophyll fluorescence (F), and merged image of (E) and (F) (all channels) (G).

Chloroplasts appear red in (A) to (D) as a result of chlorophyll autofluorescence; the chloroplasts are shown in blue in (E) to (G) for better contrast with mRFP fusion proteins. Bar = 10 μm .

chloroplast envelope (see Supplemental Figure 3 online). This allows close proximity of TPS and P450 proteins and may enable either direct trapping or transfer of TPS products possibly through hemifused membrane bilayers, as recently suggested by Mehrshahi et al. (2013). It also has to be stressed that these proteins might be localized differently in the anther filaments themselves, which are not photosynthetic tissues. Attempts to visualize the protein fusion constructs in the anther filaments of stable *Arabidopsis* transformants were not successful.

Linalool Is the Main Product of TPS10 and TPS14 Expressed in Yeast and *N. benthamiana*

Truncated versions of TPS10 and TPS14 lacking the N-terminal plastid targeting sequences were expressed in the engineered

K197G yeast strain (Fischer et al., 2011), using the same truncation sites as described by Bohlmann et al. (2000) and Chen et al. (2003), respectively. The K197G strain was chosen because it accumulates more geranyl diphosphate, the substrate for monoterpene synthases, than wild-type yeast. This is attributable to the presence of a mutated farnesyl diphosphate synthase that releases substantial amounts of geranyl diphosphate, normally an enzyme-bound reaction intermediate. Two days after induction of TPS expression, the culture medium was extracted and analyzed via gas chromatography–mass spectrometry (GC-MS). Contrary to what was previously observed after expression of TPS10 in *E. coli* (Bohlmann et al., 2000), both TPS10 and TPS14 expression in yeast led to the formation of linalool as the main product (Figures 5A1 and 5A2). TPS-dependent formation of additional minor products including myrcene and geraniol could not be reliably distinguished from yeast-dependent production of these monoterpenes.

It was previously shown that TPS products can vary depending on the recombinant organism used for expression and also with the subcellular localization of the protein (Huang et al., 2010; Fischer et al., 2013). We thus determined which TPS10 and TPS14 products are generated in planta by the untruncated and hence chloroplast-targeted versions of these proteins. The full-length TPS10 and TPS14 were transiently expressed in *N. benthamiana* leaves, and emitted volatiles were analyzed by GC-MS. TPS10-transfected leaves emitted four monoterpenes, with linalool as the main product (94%) and myrcene and (*E*)- β -ocimene formed as minor side products (Figure 5B2). By contrast, linalool was the only volatile product detected in TPS14-transfected leaves (Figure 5B1). Both TPS10 and TPS14 thus form linalool as their major or exclusive product in planta and in yeast, whether expressed as truncated or full-length proteins.

TPS10 and TPS14 Are Stereospecific Linalool Synthases

Given that TPS10 and TPS14 are expressed in the same tissues, it was important to determine whether they generated the same products. We thus examined the enantiomeric composition of the products. Standard GC does not allow differentiation of linalool enantiomers. TPS10 and TPS14 were thus expressed in *N. benthamiana* and yeast as described above, and compounds emitted from leaves or excreted into the yeast medium were analyzed on a chiral column–equipped GC-MS device. The TPS10 and TPS14 products generated from both yeast and plants were compared with authentic standards of linalool enantiomers (Figures 5C1 to 5C5). Data obtained using both expression systems show that (–)-(3*R*)-linalool was the main product of TPS10 and (+)-(3*S*)-linalool was the product of TPS14. TPS10 and TPS14 are thus not redundant and produce opposite linalool enantiomers.

CYP76C3 and CYP71B31 Metabolize Linalool

To test our hypothesis that CYP76C3 and CYP71B31 use the TPS10 and TPS14 product linalool as a substrate, TPS10 was transfected into *N. benthamiana* leaves alone or in combination with CYP76C3 or CYP71B31. Upon simultaneous expression of multiple protein-GFP constructs, as reported above, we consistently observed a significant reduction in the expression of each individual protein fusion. TPS10 was thus also coexpressed with CYP98A3

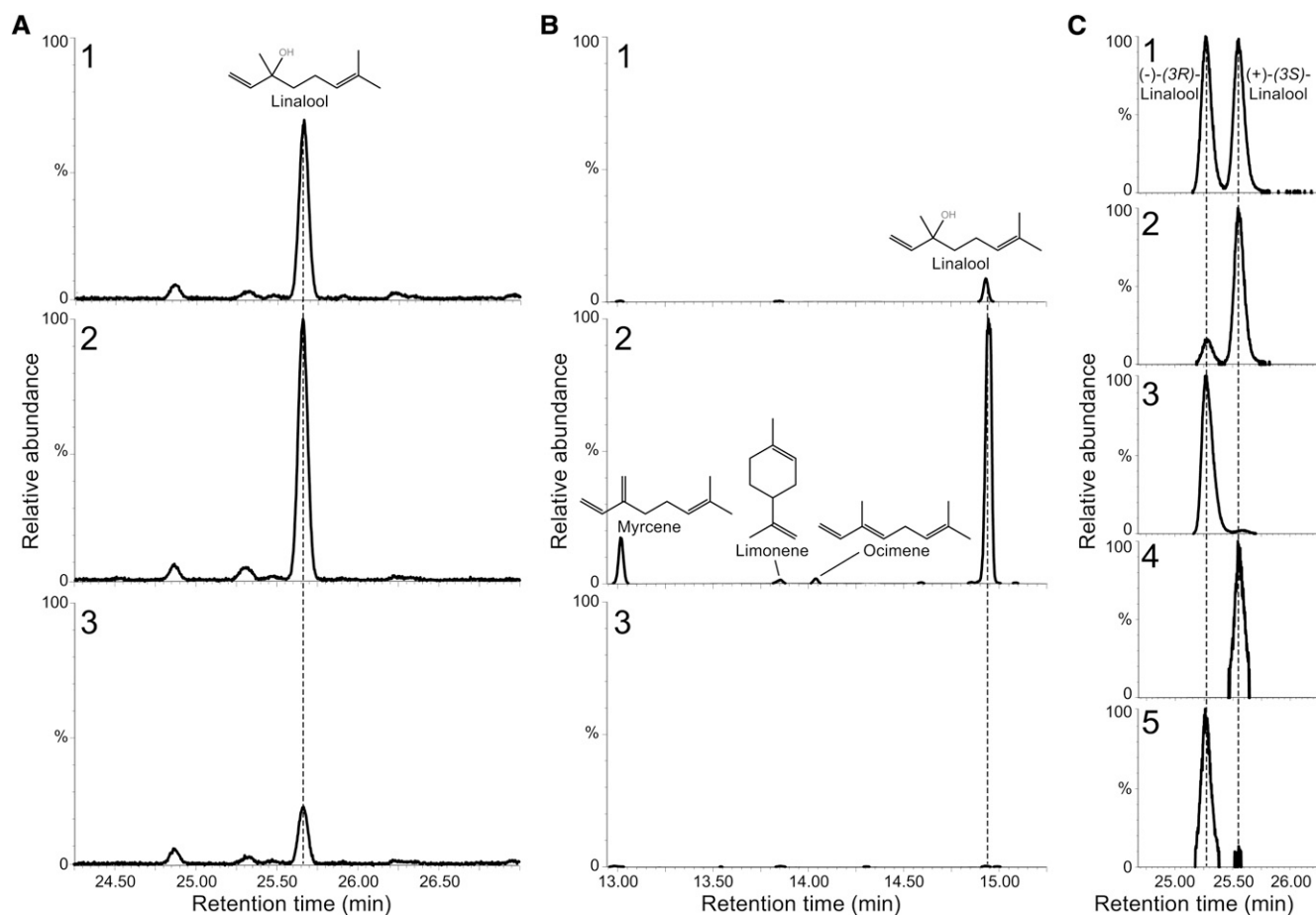


Figure 5. Products of the Heterologously Expressed Monoterpene Synthases TPS10 and TPS14 Depicted in Gas Chromatograms.

(A) Products of the yeast-expressed enzymes extracted by SPE from 120 mL culture medium of $OD_{600} = 10$. Depicted is a section of a GC-MS trace of m/z 93, a major ion in the spectra of linalool and most monoterpene olefins: TPS14 (**1**), TPS10 (**2**), and empty vector-transformed yeast (**3**). A small amount of linalool is produced by K197G yeast.

(B) Volatiles collected 5 d after transformation of *N. benthamiana* leaves with TPS14 (**1**), TPS10 (**2**), and empty vector control (**3**). GC-MS depicted as in **(A)**. **(C)** Chiral analysis of racemic linalool standard (**1**) and the linalool produced by TPS14 (**2**) or TPS10 (**3**) in yeast or by TPS14 (**4**) or TPS10 (**5**) in *N. benthamiana*. GC-MS depicted as in **(A)**.

(the phenolic ring meta-hydroxylase in the phenylpropanoid pathway) (Schoch et al., 2001; Franke et al., 2002) as a negative control. The amount of linalool produced by TPS10 was three times lower when coexpressed with CYP98A3 than when TPS10 was expressed alone (Figure 6). However, the amount of linalool emitted when TPS10 was coexpressed with CYP71B31 instead of CYP98A3 was significantly further reduced, and even more so when coexpressed with CYP76C3. This indicates that (+)-(3S)-linalool was metabolically converted by both CYP76C3 and CYP71B31. An analysis of the leaf volatiles using headspace GC-MS, however, did not detect oxidized linalool products, most likely because of the reduced volatility of these products or their further conjugation.

CYP76C3 and CYP71B31 Convert Linalool into Different Oxygenated Products

To identify the actual CYP76C3 and CYP71B31 linalool conversion products, both P450 enzymes were expressed in the WAT11

and WAT21 yeast strains expressing *Arabidopsis* P450 reductases ATR1 and ATR2, respectively. In spite of the functional expression of CYP76C4 (Höfer et al., 2013) run in parallel in the same experiment, no functional P450 enzyme could be detected in the microsomal membranes harvested from transformed yeast cultures based on spectrophotometric evaluation of the CO-reduced enzyme. Accordingly, no significant linalool transformation was observed in in vitro enzyme assays conducted using preparations of these yeast microsomes. We thus explored a plant expression system and CYP76C3 and CYP71B31 were transfected into *N. benthamiana* leaves. After 4 d (which leads to optimal P450 expression, according to the above-described protein:GFP fusion expression experiments), leaf discs were fed the two linalool enantiomers separately, and products excreted by the leaf discs were analyzed using GC-MS. Both P450 enzymes catalyzed the formation of several products (Figures 7 and 8). Peaks were identified either based on comparison of the mass spectra with authentic standards, or

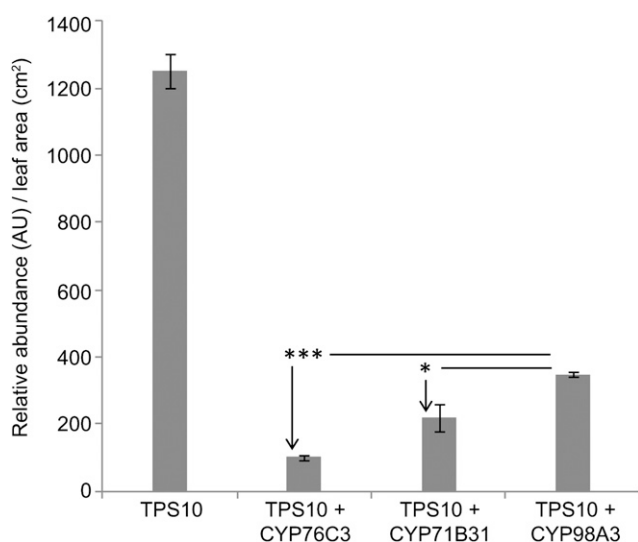


Figure 6. Linalool Emission from Leaves of *N. benthamiana* Transformed with *TPS10* Declines when Leaves Are Cotransformed with *CYP76C3* or *CYP71B31*, Suggesting That Linalool Is Metabolized by both P450 Enzymes.

CYP98A3 is used as a negative control to evaluate the decline in *TPS10* expression upon coexpression of any second gene. Coexpression with *CYP98A3* causes a decline in *TPS10* product, but linalool emission declines further when *TPS10* is coexpressed with either *CYP76C3* or *CYP71B31*. Linalool emission was quantified by GC-MS analysis of collected volatiles. Error bars indicate SE. $n = 3$. * $P < 0.05$; *** $P < 0.001$.

through nuclear magnetic resonance (NMR) structure determination of purified compounds.

All of the products formed were oxygenated derivatives of linalool, but the product spectrum for each enzyme was distinct, varying with the chirality of the linalool substrate administered. *CYP71B31* catalyzed the formation of four products when fed (3*S*)-linalool, with (3*S*)-1,2-epoxylinol and diastereomers (3*S*,5*S*)-hydroxylinol and (3*S*,5*R*)-hydroxylinol being the major products accompanied by a trace of (3*R*)-4-hydroxylinol (Figure 7A). By contrast, (3*R*)-linalool gave rise to (3*S*)-4-hydroxylinol and diastereomers (3*R*,5*S*)-hydroxylinol and (3*R*,5*R*)-hydroxylinol, the most abundant of the two having identical chirality on carbon 5 as when (3*S*)-linalool was used as substrate (Figure 7D). No 1,2-epoxylinol was detected.

CYP76C3 catalyzed the formation of a somewhat different set of products than *CYP71B31*, with 8-hydroxylinol and an unknown linalool derivative with oxygenation at position eight or nine being formed instead of 1,2-epoxylinol and 4-hydroxylinol (Figures 7B and 7E). In addition, *CYP76C3* produced the same two diastereomers of 5-hydroxylinol as *CYP71B31* with similar relative proportions.

To further investigate the substrate specificity of *CYP76C3* and *CYP71B31*, geraniol, nerol, myrcene, and ocimene were also tested as substrates with transfected *N. benthamiana* leaf discs, but no oxygenated products were detected in the incubation buffer extracts. Because linalool is selectively metabolized by both enzymes, we also considered the possibility that *CYP76C3* and

CYP71B31 could catalyze successive steps in linalool metabolism. *N. benthamiana* was thus simultaneously cotransfected with *CYP76C3* and *CYP71B31*, and leaf discs were incubated with linalool. No additional products were detected in incubation buffer extracts compared with discs transformed with single constructs upon GC-MS analysis. However, we cannot completely exclude the formation of more oxygenated compounds because no liquid chromatography–mass spectrometry analysis of the extract was performed.

Effect of Candidate Genes on the Flower Metabolic Profile of *Arabidopsis*

In an attempt to determine the influence of the four genes on flower development and the production of linalool-derived metabolites in flower tissues, two homozygous T-DNA insertion lines were obtained and validated by PCR screening. For *TPS14*, only one line could be confirmed (see Supplemental Figure 4 online). Although lack of gene expression was confirmed in all insertion mutants, no alteration in flower development, morphology, or fertility was observed. GC-MS analyses of the headspace collected from blooming inflorescences detected no significant residual emission of linalool in the *tps10 tps14* double mutant (see Supplemental Figure 5 online), indicating that no other linalool synthase was expressed in the flower tissues. A small but significant (~30%) increase in the emitted linalool was observed for the *cyp76c3* mutant (see Supplemental Figure 6 online), but we did not detect significant changes in any volatile oxygenated linalool derivatives.

This raised the possibility that the oxygenated linalool products of *CYP71B31* and *CYP76C3* were further metabolized. Aharoni et al. (2003) reported the accumulation of glycosylated 8-hydroxylinol in *Arabidopsis* leaves transformed with a strawberry linalool synthase, and small amounts of glycosylated hydroxylinol were detected in the leaves of the wild-type plants. In addition, the formation of monoterpenol glycosides was reported in rosebuds (Francis and Allcock, 1969) and flowers from *Clarkia breweri* (Raguso and Pichersky, 1999). Blooming inflorescences from *Arabidopsis* wild-type and mutant lines were therefore methanol extracted for untargeted profiling using ultrahigh performance liquid chromatography–mass spectrometry (UHPLC-MS) (Orbitrap). In a second approach, a targeted analysis of the same extracts was performed using ultra performance liquid chromatography–tandem mass spectrometry (UPLC-MS/MS) in multiple reaction monitoring (MRM) mode targeting ions corresponding to linalool, 8-hydroxylinol, 8-oxo-linalool, 8-carboxylinalool, and 1,2-epoxylinol.

Untargeted analyses identified 13 conjugates of monoterpene oxides in the wild-type flowers. Exact masses of each peak were consistent with linalool oxide moieties present mainly as hexose and malonyl hexose conjugates (see Supplemental Figure 7 online). Ten of the aglycone moieties of these compounds are likely oxidized once, and two of them twice. Four of them are hexose conjugates and five are malonyl hexose adducts. Their structures could not be elucidated because of their low amounts and unavailability of reference compounds, but could be narrowed down to a few possibilities (see Supplemental Figure 7 online). Eight of these conjugates had an aglycone moiety of identical mass that could correspond to either 1,2-epoxylinol

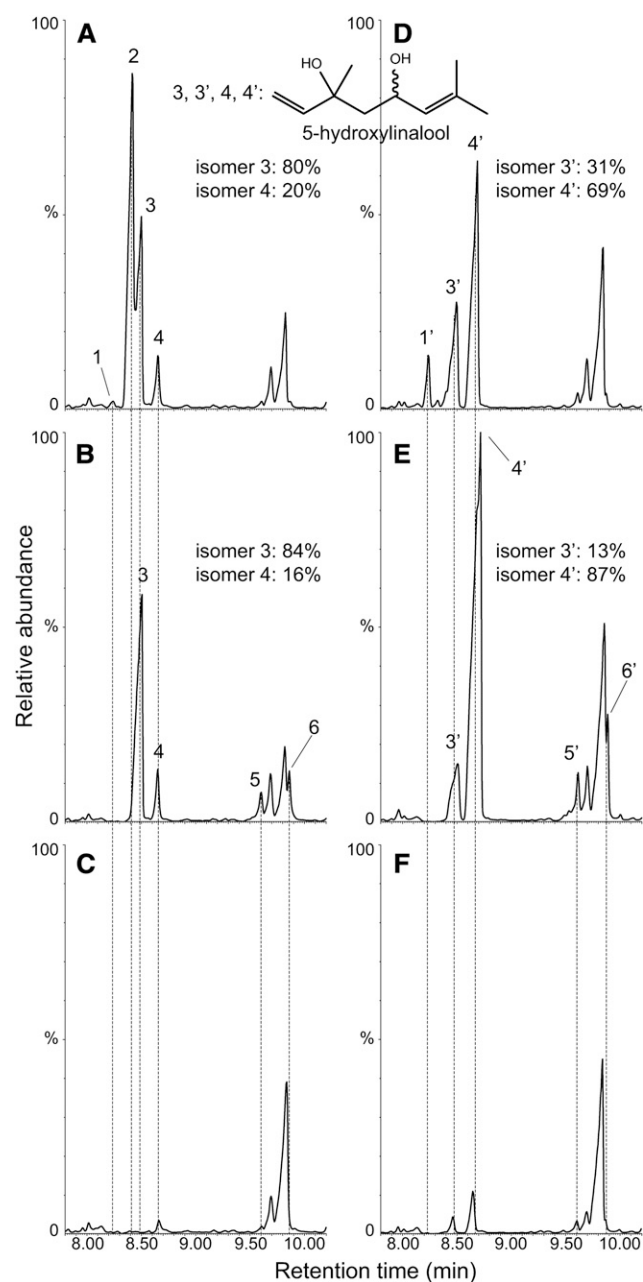


Figure 7. Enzymatic Products of P450s CYP76C3 and CYP71B31 after Administration of Linalool Enantiomers to *Agrobacterium*-transformed *N. benthamiana* Leaf Discs.

Leaves were infiltrated with *Agrobacterium* transformed with an empty vector or with vectors driving expression of CYP76C3 or CYP71B31. Leaf discs (22 discs, 11 mm diameter) were excised 5 d postinfiltration and incubated 4 h in buffer containing 200 μ M linalool. A pentane:ethyl acetate (4:1) extract of the incubation buffer was analyzed on a GC-MS device, and the chromatograms are depicted here. (S)-linalool was used as the substrate in (A) to (C), and (R)-linalool was used as the substrate in (D) to (F).

(A) and (D) CYP71B31-infiltrated leaves.

(B) and (E) CYP76C3-infiltrated leaves.

(C) and (F) empty vector control.

or 6,7-epoxylinalool, hydroxyl-linalool (with hydroxylation at any position), lilac alcohol, linalool oxide, or 6-hydroxy-8-oxo-linalool. Whereas amounts of several of these compounds varied in the insertion mutants, none of them was totally suppressed, and the method was not suitable for reliable comparison of their concentrations in the different samples.

The targeted analysis identified several compounds significantly decreased or increased in the TPS or P450 mutants with retention times distinct from the free aglycones of the targeted compounds (Figure 9). Hexose and malonyl hexose conjugates of linalool were significantly decreased in the *tps* null mutants and increased in the *cyp76C3* mutant lines, consistent with linalool production by TPS10 and TPS14 and linalool metabolism by CYP76C3 in vivo, whereas the most abundant oxygenated compound 8-hydroxy-linalyl Glc decreased in both *tps* mutants and increased in the *cyp76c3* mutant. This may be explained by redirection of linalool for metabolism via competing oxygenase(s) with 8-hydroxylase activity. By contrast, *cyp71b31* mutants displayed no significant changes in the metabolites targeted, which suggests a minor role in linalool metabolism in vivo or channeling to different products. Interestingly, two peaks with a $m/z = 137$ fragment (expected from linalool and derivatives) but different retention times were fully absent in both *tps10* and *cyp76c3* knockout lines (Figure 9), indicating coupling of the two enzymes for the formation of this compound. The compound was present in insufficient amounts for unambiguous identification. However, the complete suppression of this compound in *tps10* and *cyp76c3* knockout lines indicates that there is no TPS/CYP redundancy for its formation in the plant.

DISCUSSION

The monoterpene alcohol, linalool, is present in the floral scent emitted by many moth- and bee-pollinated plants (Raguso and Pichersky, 1999). Flowers from plants producing linalool usually also emit linalool oxides (Pichersky et al., 1994; Kreck et al., 2003; Matich et al., 2011). *Arabidopsis* is an essentially autogamous plant and its flowers are reported to emit only extremely low amounts of linalool and oxygenated derivatives (Chen et al., 2003; Rohloff and Bones, 2005). It was thus rather unexpected that our in silico coexpression analysis approach, aimed at plant P450 functional characterization and identification of genes contributing to common metabolic networks, revealed complex floral linalool metabolism in *Arabidopsis*. The four genes we selected for their highly correlated expression, encoding two linalool synthases (TPS10 and TPS14) and two P450 enzymes (CYP71B31 and CYP76C3), participate in this metabolism and contribute to the production of a complex blend of oxygenated linalool derivatives. These compounds then appear to be further processed and stored in the floral tissues as conjugated oxides.

All four genes are mainly expressed in flowers, and their expression starts shortly before anthesis. A detailed analysis of

The following products are shown: 4-hydroxylinalool (1), 1,2-epoxylinalool (2), 5-hydroxylinalool (3, 3' and 4, 4'), 8-oxo-linalool or 9-hydroxylinalool (5a, 5a' and 5b, 5b'), and 8-hydroxylinalool (6, 6'). For summaries of the activities of each enzyme, see Figure 8.

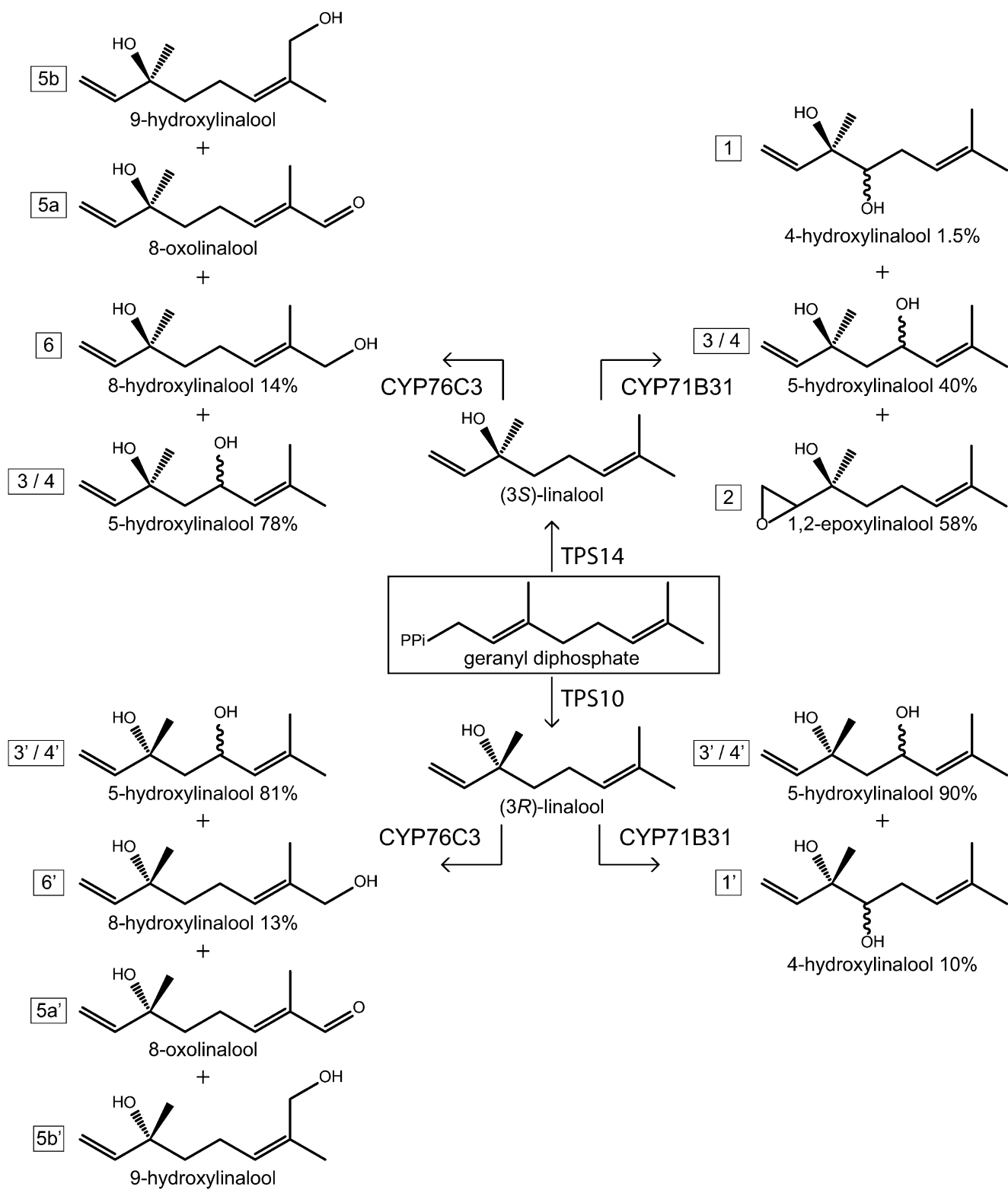


Figure 8. Scheme Summarizing the Catalytic Activities of the Characterized Monoterpene Synthases (TPS10 and TPS14) and P450s (CYP76C3 and CYP71B31).

Calculation of the percentage of products for each enzyme is based on triplicate assays analyzed by GC-flame ionization detection. Peak correspondence with Figure 7 is indicated in squares.

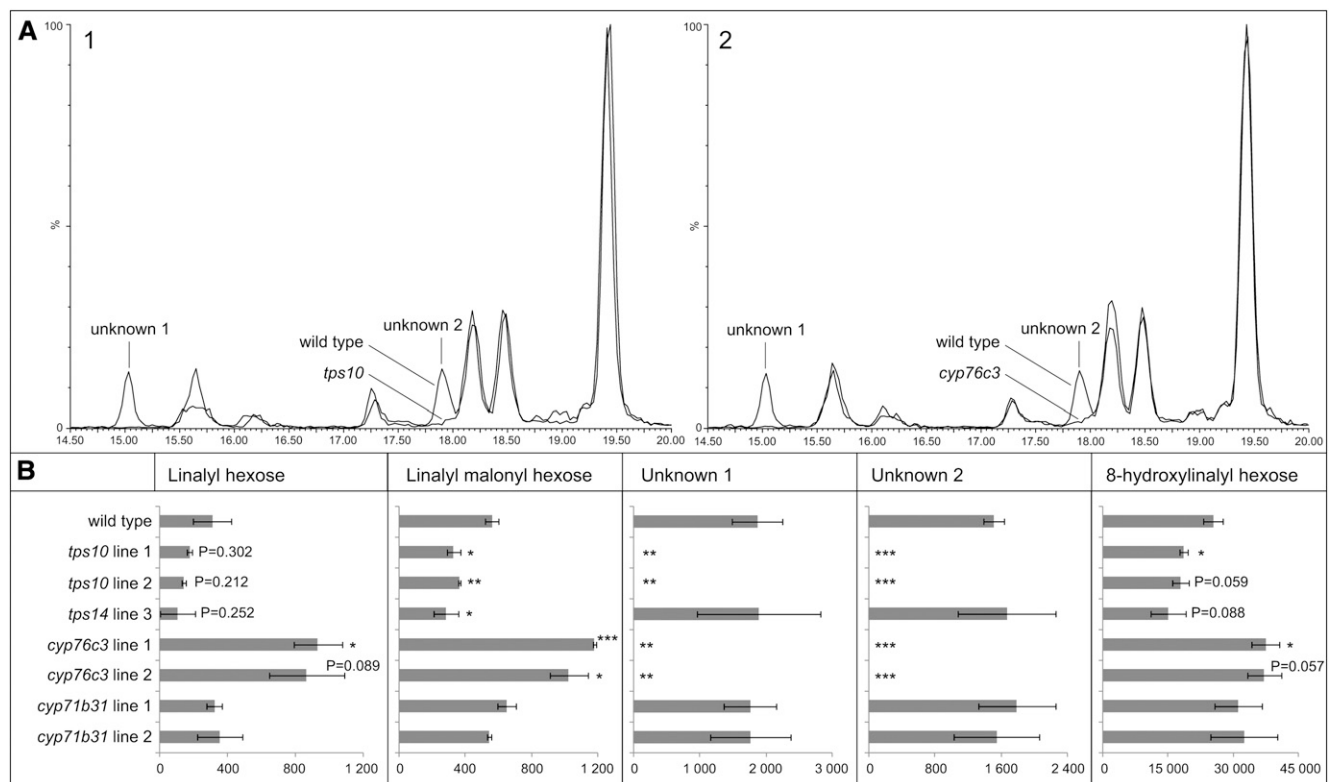


Figure 9. Targeted UPLC-MS Analysis of Linalool Derivatives in the Wild Type and TPS/P450 Insertion Mutants.

(A) Overlaid UPLC-MS chromatograms of the wild type versus the *tps10* null mutant **(1)**, and the wild type versus the *cyp76c3* null mutant **(2)**. Two compounds are missing from the mutant flower methanol extracts.

(B) Relative abundance of relevant monoterpenoid conjugates in the flower methanol extracts of *Arabidopsis* null mutants. Error bars indicate se. $n = 3$. * $P < 0.05$; ** $P < 0.01$; *** $P < 0.001$.

gene promoter activity shows that both linalool synthases and linalool oxidases are simultaneously expressed in the same floral organs, mainly in the upper half of the anther filament and petals. This tight coexpression pattern suggests a coupling of linalool production and oxidation in these tissues, and may explain why only traces of free linalool are detected in the *Arabidopsis* floral headspace analysis. The highest expression in the tip of the filament also suggests a possible transfer of some final products to the anther tissues. The small amount of free linalool that can be collected from the open flowers possibly results from the TPS expression in the receptacle, where no CYP76C3 and CYP71B31 expression is detected. Conversely, the two linalool oxidases are found expressed in the nectaries, where TP10 and TPS14 are not expressed, which suggests that either their substrate in this organ is formed by another TPS or that linalool is transported from the receptacle, petal, or anther tissues.

TPS10 was previously described as a β -myrcene and (*E*)- β -ocimene synthase (Bohlmann et al., 2000) based on the *in vitro* activity of a truncated protein in *E. coli*. However, in our hands, TPS10 expression in yeast and *N. benthamiana* led to an enzyme with ($-$)-(3*R*)-linalool as a main product and β -myrcene and (*E*)- β -ocimene as minor side products. The (+)-(3*S*)-linalool enantiomer was determined to be the main product of TPS14. In both cases,

we expressed truncated and full-length proteins and obtained the same products. This points to the importance of the choice of recombinant organisms for the functional characterization of TPS enzymes (Fischer et al., 2013). Analysis of the *Arabidopsis* floral volatiles confirmed TPS10 and TPS14 production of linalool, because no residual linalool is emitted by the *tps10 tps14* double mutant and a small but significant increase in linalool emission was observed in the loss-of-function mutants of CYP76C3. From a phylogenetic point of view, TPS10 and TPS14 are not closely related paralogs, but belong to two different clades of TPS proteins (Aubourg et al., 2002). Their capacities to form linalool thus evolved independently. Accordingly, TPS10 selectively forms ($-$)-(3*R*)-linalool, whereas TPS14 produces (+)-(3*S*)-linalool.

P450s are often described as stereospecific enzymes. It was therefore surprising to observe that both CYP71B31 and CYP76C3 metabolized both ($-$)-(3*R*) and (+)-(3*S*) enantiomers of linalool. Functional enzymes were obtained in plant tissues but not in yeast microsomes. Successful expression of active enzymes in yeast was previously obtained for related P450s under the same conditions (Höfer et al., 2013), suggesting that CYP76C3 and CYP71B31 proteins might be unstable in yeast, either attributable to membrane context or to interaction with yeast metabolites. Consequently, it was not possible to compare their catalytic efficiencies with regard

to linalool enantiomers. CYP71B31 and CYP76C3 belong to the same CYP71 clan that usually metabolizes small molecules, but to different families of P450 enzymes. Their linalool oxygenase activities thus also result from independent evolution.

Whereas TPS10 and TPS14 and CYP71B31 and CYP76C3 are coexpressed in the same plant tissues, they do not colocalize in the same subcellular compartments when expressed as eGFP fusions in the *N. benthamiana* leaf epidermis. Both TPS10 and TP14 are associated with the plastids as expected from their predicted N-terminal transit peptide, but they are not detected in the stroma or stroma-containing plastidial extensions described as stromules (Mathur et al., 2012). They instead appear concentrated in vesicular structures located at the inner or outer surface of the plastids. This localization distinguishes them from the lipoprotein particles described as plastoglobules, associated with the thylakoids (Austin et al., 2006; Bréhélin and Kessler, 2008), but their role in sequestration and possibly channeling of reactive and potentially toxic hydrophobic compounds between membranes might be similar. Interestingly, overexpression of markers of the inner envelope was also reported to induce the formation of plastid-associated punctate structures (Breuers et al., 2012). When simultaneously expressed in fusion with different fluorescent proteins, TPS10 and TPS14 colocalized in the same vesicles (Figures 4E to 4G). Colocalization and direct protein–protein interaction would be expected to favor TPS and P450 cooperation and substrate channeling in a linalool pathway, but CYP76C3 and CYP71B31 show a clear association with the ER membranes. The plastids, however, appear to nest in a cradle of the ER network. The existence of direct contact sites between the ER and the plastidial envelope was demonstrated (Andersson et al. (2007) and is also suggested by images collected upon P450 and TPS coexpression (see Supplemental Figure 2 online). Transorganellar plastid:ER transfer of metabolites was recently confirmed (Mehrshahi et al., 2013). A concentration of the linalool synthases in lipoprotein structures at the plastid surface should favor linalool sequestration and transfer to the adjacent ER membranes where the P450 linalool oxidases reside, thus limiting the emission of free linalool or its conjugation in the cytoplasm.

The extensive linalool metabolism in *Arabidopsis* flowers raises questions about its function. Linalool is a well-documented flower attractant for pollinators, but most of the linalool produced by *Arabidopsis* flowers seems to be further converted into oxidized derivatives. Although flower visitors to this species have been reported in wild populations (Hoffmann et al., 2003), *Arabidopsis* is considered an autogamous plant. Thus, the linalool derivatives in this species seem unlikely to be functioning as attractants for pollinators. In fact, no significant change was found in the emission of volatile linalool oxides from the flowers of the *cyp76c3* and *cyp71b31* mutant lines. Moreover, the formation of nonvolatile, most soluble conjugates of linalool oxides was not suppressed in these single mutants. Coexpression analysis indicates that other P450 enzymes belonging to the CYP71 and CYP76 families (http://www.ibmp.u-strasbg.fr/~CYPedia/CYP76C3/CoExp_CYP76C3_Organs.html) are coregulated with CYP76C3. If these also metabolize linalool, they may mask changes induced by CYP76C3 and CYP71B31.

The main role of linalool metabolism in *Arabidopsis* flowers may be to produce the nonvolatile, oxygenated linalyl conjugates we detected by UPLC-MS. These compounds are expected to accumulate mainly at the sites of gene expression, including anther

filaments, petals, and nectaries. Hence, one possible function of linalool metabolism might be the production of antioxidants to protect these organs from damage until fertilization takes place (Jerković and Marijanović, 2010). However, knockout mutants of the linalool-oxidizing P450s we studied did not exhibit any changes in floral development, morphology, or fertility. A second possible function of oxygenated linalool derivatives and their conjugates might be in the defense against pathogens and insect herbivores (Herken et al., 2012). Other terpene volatiles emitted from *Arabidopsis* flowers have been demonstrated to function in protection against pathogen attack (Huang et al., 2012). A third possibility is that linalool metabolism serves to detoxify linalool, which is active in plant defense but is also cytotoxic (Erdogan and Ozkan, 2013; Maietti et al., 2013).

Whatever the role of linalool metabolism in *Arabidopsis* flowers, further transformation of this monoterpene alcohol may be a more general phenomenon in vascular plants. Linalool itself is an extremely widespread floral volatile (Knudsen et al., 2006), and the sequestration of linalool derivatives or derivatives of the isomeric monoterpene alcohol geraniol has been reported in the floral organs of several unrelated plant species (Francis and Allcock, 1969; Watanabe et al., 1994; Raguso and Pichersky, 1999). Because linalool and derivatives are also present in substantial amounts in the reproductive structures of more primitive plants, such as cycads (Terry et al., 2004) and members of the Winteraceae (Pelmyr et al., 1990), and the CYP76 and CYP71 P450 families are represented in all seed or flowering plants, respectively (Nelson and Werck-Reichhart, 2011), the P450-dependent formation of oxygenated derivatives of monoterpene alcohols might have been an early protective feature of reproductive structures in seed plants.

METHODS

Plant Growth

Seeds of *Arabidopsis thaliana* and *Nicotiana benthamiana* were sown on a standard soil compost mixture, and seedlings were grown individually in growth chambers under white fluorescent lamps under a photon fluency of 40 to 60 $\mu\text{mol} \cdot \text{m}^{-2} \cdot \text{s}^{-1}$ at the rosette level and 70 to 90 $\mu\text{mol} \cdot \text{m}^{-2} \cdot \text{s}^{-1}$ at the *Arabidopsis* inflorescence tips. The temperature was 22°C during the 12-h day period and 19°C during the 12-h night period for *Arabidopsis*, and 24°C during the 16-h day period and 20°C during the 8-h night period for *N. benthamiana*.

Synthesis of 8-Hydroxylinalool and 8-Oxo-Linalool

Following a slight modification of the procedure of Sharma and Chand (1996), a solution of linalool (1.30 g, 8.42 mmol), in CH_2Cl_2 (10 mL) was added dropwise to a stirred mixture of selenium dioxide (94 mg, 0.85 mmol) and 75% tert-butyl hydroperoxide (3 mL, 25.2 mmol in 25 mL CH_2Cl_2) at 15°C and stirred for 5 h. The reaction mixture was diluted with ether (100 mL), and then 10% aqueous KOH was added and the layers were separated. Subsequently, water and then saturated aqueous NaCl were added in sequence to the ether solution, and each time the aqueous layer was separated from the organic layer. The resulting ether solution was dried over anhydrous sodium sulfate. After concentration in vacuo, purification of the residue by column chromatography (petroleum ether, EtOAc) afforded (+)-(E)-2,6-dimethyl-6-hydroxy-octa-2,7-dienal (72 mg, 0.43 mmol, 5%) and (+)-(E)-2,6-dimethylocta-2,7-diene-1,6-diol (1.02 g, 5.99 mmol,

71%). Both compounds displayed identical spectroscopic data to those previously reported (Wilkins et al., 1993; Sharma and Chand, 1996; Singh et al., 2009). Treatment of (+)-(E)-2,6-dimethyl-6-hydroxy-octa-2,7-dienal with NaBH₄ in methyl alcohol afforded (+)-(E)-2,6-dimethylocta-2,7-diene-1,6-diol following the procedure of Sharma and Chand (1996).

RNA Extraction and qRT-PCR

Fresh material was harvested from at least five different plants and immediately frozen in liquid nitrogen. Total RNA was precipitated and extracted with lithium chloride-phenol, treated with DNase I (Fermentas), and further purified with the RNeasy plant mini kit (Qiagen) according to the manufacturer's instructions. cDNA was synthesized with SuperScript III Reverse Transcriptase (Invitrogen) in the presence of Oligo(dT)23 (Sigma-Aldrich Chemie) from 2 µg total RNA and resulting cDNA was diluted 10-fold. The quantitative PCR cycle threshold (Ct) values were normalized to the Ct values obtained for four reference genes whose stable expression in *Arabidopsis* tissues is known as follows: *SAND* (At2g28390), *TIP41* (At4g34270), *PP2A* (At1g13320), and *EXP* (At4g26410) (Czechowski et al., 2005). Oligonucleotides used for each gene are provided in Supplemental Table 1 online. Relative expression was calculated with the specific efficiency of each primer pair by using the E_ΔCt method (Pfaffl, 2001). Five biological replicates were used for the organs, three for the flower stages, and four for the flower parts.

Generation of Expression Vectors

The yeast and plant expression constructs were generated by PCR amplification of the desired fragment from cDNA prepared from flower tissues of *Arabidopsis* with primers harboring the appropriate Uracil-Specific Excision Reagent (USER; New England Biolabs) extension (see Supplemental Table 1 online). The USER cloning technique was used according to Nour-Eldin et al. (2006) to integrate the PCR fragments into the yeast expression plasmid pYeDP60u2 (Höfer et al., 2013) and plant expression vector pCAMBIA2300u (for transient expression in *N. benthamiana* leaves and overexpression in *Arabidopsis*). Constructs were confirmed by sequencing.

Determination of Tissue-Specific Gene Expression

A 1.5-kb promoter region of each candidate gene was isolated by PCR from *Arabidopsis* genomic DNA using appropriate primers (see Supplemental Table 1 online). The resulting PCR products were integrated into the plant pBI101u expression vector modified to harbor a USER cloning cassette upstream of *GUS* (*uidA*) (Schlaman et al., 1994). Constructs were confirmed by sequencing. The constructs were introduced into the GV3101 *Agrobacterium tumefaciens* strain, which was used to transform *Arabidopsis* by floral dip (Clough and Bent, 1998). Transformed lines were selected on plate containing 50 µg·mL⁻¹ kanamycin and 100 µg·mL⁻¹ cefotaxime, and were confirmed by PCR after genomic DNA extraction. Enzymatic assays with 5-bromo-4-chloro-3-indolyl-β-D-glucuronide were performed for localization of GUS activity (Jefferson et al., 1987).

Determination of the Subcellular Localization of the Candidate Proteins

The cDNA of the enhanced GFP (Sagt et al., 2009) or of the monomeric RFP (Campbell et al., 2002) was amplified and fused to the 3' end of the full-length cDNA of the candidate genes according to the method of Geu-Flores et al. (2007), using primers in Supplemental Table 1 online. The stop codon of the candidate genes was removed and replaced by a codon for Gly followed by the ACCGGTCGCCAC sequence encoding the TGRH linker peptide to ensure flexibility of the protein junction. The resulting PCR products were cloned into the vector pCAMBIA2300u adapted with a USER cassette (Nour-Eldin et al., 2006) under control of the cauliflower

mosaic virus-35S promoter. Vector for the ER marker expression of mRFP:HDEL was kindly provided by C. Ritzenthaler (Boulaflous et al., 2009). The constructs were transformed into the hypervirulent *Agrobacterium* LBA4404 strain and transformed agrobacteria were grown at 28°C for 30 h in 5 mL liquid Luria-Bertani medium containing 25 µg·mL⁻¹ rifampicin, 25 µg·mL⁻¹ gentamicin, and 50 µg·mL⁻¹ kanamycin. Bacteria were harvested and washed twice in distilled water. Cultures with an OD₆₀₀ = 0.4 were mixed with a culture of equal density expressing the candidate protein:p19 protein of tomato bushy stunt virus (Voinnet et al., 2003) in a ratio of 4:1 (v/v) and 2:2:1 (v/v/v) for coexpression of P450:HDEL:p19. The mixture of agrobacteria was used for the infiltration of two leaves of 39-d-old *N. benthamiana*. Four days after infiltration, leaves were detached and used for image acquisition with a LSM510 confocal microscope (software version AIM 4.2; Carl Zeiss), using a ×63, 1.2 numerical aperture water immersion objective lens at 23°C. Fluorescence of free eGFP/mRFP, eGFP/mRFP fusion proteins, or chloroplasts was observed after excitation with 488 nm (eGFP and chlorophyll) or 561 nm (mRFP) laser lines, and using 505 to 550 nm band-pass (eGFP), 560 nm low-pass (chlorophyll), or 575 to 615 nm band-pass (mRFP) emission filters.

Heterologous Expression in Yeast

Yeast expression constructs were transformed into the K197G yeast strain (Fischer et al., 2011) as described by Gietz and Schiestl (2007). A transformed colony was grown in 10 mL selection medium (standard minimum medium consisting of 6.7 g/L yeast nitrogen base without amino acids and 2% Gal, supplemented with Leu, Trp, and His) for 48 h at 28°C. This preculture was used to inoculate a 120 mL culture consisting of the same medium at an initial OD₆₀₀ = 0.15. Gal 2% was used as a carbon source and inducer. The medium was set at pH 7.0 with 50 mM phosphate-citrate buffer and checked at the end of the culture. After 48-h culture at 28°C, the excreted products were extracted using solid phase extraction cartridges (Oasis HLB 3 cc, 60 mg, extraction cartridges; Waters), which had been sequentially equilibrated with ethyl acetate, methanol, and water, prior to gradual extraction of up to 60 mL yeast culture supernatant. After drying, the cartridges were eluted with 2.5 mL ethyl acetate, and the combined organic phase was dried over Na₂SO₄, concentrated in a stream of argon to ~200 µL before GC-MS analysis.

Yeast Microsome Isolation and Enzyme Assay

The WAT11 yeast strain was transformed with pYeDP60u2 harboring the CYP76C3 or CYP71B31 sequences as described (Gietz and Schiestl, 2007). Transformant cultivation and induction as well as preparation of yeast microsomes were performed according to the method described in Gavira et al. (2013). P450 expression in yeast microsomes was evaluated by differential spectrophotometry according to the method described by Omura and Sato (1964). Enzyme assays were performed as described by Höfer et al. (2013).

Transient Expression in *N. benthamiana* and Collection of Emitted Volatiles

Plant expression constructs were transformed into the hypervirulent *Agrobacterium* LBA4404 strain. The transformed agrobacteria were grown at 28°C for 30 h in 5 mL liquid Luria-Bertani medium containing 25 µg·mL⁻¹ rifampicin, 25 µg·mL⁻¹ gentamicin, and 50 µg·mL⁻¹ kanamycin. Bacteria were harvested, washed twice in distilled water, and cultures of an OD₆₀₀ = 0.4 expressing the TPS:P450:p19 protein were mixed in a 2:2:1 ratio v/v/v. In the control, the culture harboring the P450 plasmid was replaced with water. Young, fully expanded leaves of 5-week-old *N. benthamiana* plants were infiltrated on the abaxial side with the bacterial mix using a needleless syringe. Four days after infiltration, two to four infiltrated leaves were detached and gathered as a bouquet in a small vial filled with 4 mL water.

Leaf headspace was sampled according to the procedure described by Aharoni et al. (2003). Each leaf sample with petioles dipped in a water-

filled glass vial was placed in a 1-liter glass jar fitted with a Teflon-lined lid equipped with an inlet and an outlet. A vacuum pump was used to draw air through the glass jar at ~100 mL/min. The incoming air was purified through a metal cartridge (140 mm length, 4 mm diameter) containing 200 mg Tenax TA (20/35; Grace Scientific). The volatiles emitted by the flowers were trapped at the outlet on a similar Tenax cartridge. Volatiles were sampled for 4 h. Tenax cartridges were analyzed on a PerkinElmer Clarus 680 equipped with a Perkin Elmer Clarus 600T quadrupole mass spectrometer and a TurboMatrix 100 thermal desorber (TDS) (PerkinElmer). Tenax cartridges were first dry-purged with helium at 50 mL/min for 3 min at ambient temperature to remove any water in the TDS. Volatiles were released from Tenax traps using a thermal desorption cold trap setup by heating at 250°C for 5 min, with a He flow of 50 mL/min. Desorbed volatiles were then transferred to an electronically cooled focusing trap at -30°C within the TDS. Volatiles were injected on the Perkin Elmer GC-MS device described below in 1/6 split mode into the analytical column by heating the cold trap to 280°C. Compounds were separated on a HP5-MS column (30 m × 0.50 mm i.d. × 0.5 μm thickness; Agilent Technologies).

Alternatively, for chiral analysis of TPS products, the products were eluted from the cartridge with 3×1 mL pentane:diethyl ether (v/v, 4:1) spiked with 5 μM 3-octanol as an internal standard. The organic phase was concentrated in a stream of argon to ~200 μL before GC-MS analysis.

Leaf Disc Assay

Candidate P450s were transiently expressed in *N. benthamiana* leaves as described above with *Agrobacterium* cultures mix ratios P450:p19 of 4:1 (v/v). Four days after infiltration, leaves were detached and discs (11 mm diameter) were excised with a cork borer. Five discs per leaf were incubated 4 h in a glass Petri dish, floating at the surface of 15 mL PBS buffer 20 mM, pH 7.4 containing 200 μM (*R*)- or (*S*)-linalool. Ten mL of the buffer was then liquid-liquid extracted with 10 mL pentane:ethyl acetate (v/v, 4:1) spiked with 1 μM 3-octanol. The organic phase was concentrated in a stream of argon before GC-MS analysis.

Flower Volatiles Collection and Flower Extraction for Analysis

Fifteen plants per insertion mutant line and the wild type were cultivated under short-day conditions until flowering. Three replicates with five plants per replicate were used for headspace collection. Approximately 60 inflorescences per line and per replicate were gathered as a bouquet and placed in a small glass vial filled with 4 mL water. Volatile compounds emitted were collected on Tenax-containing cartridges as described above for 24 h. Tenax cartridges were analyzed on the TDS-equipped GC-MS as described above.

After volatile collection, open flowers were cut from the inflorescences, weighed, ground, and extracted without freezing in 5 mL methanol spiked with 10 μM citronellol and using a mortar and a pestle. After 1-h incubation, the solvent was recovered, centrifuged at 3500g for 4 min to remove cell debris, and concentrated under argon to ~500 μL. The concentrate was stored at -30°C for 24 h to precipitate proteins, centrifuged at 5000g for 5 min, and the supernatant was analyzed via UPLC-MS.

GC-Flame Ionization Detection and GC-MS

Capillary GC was performed on a Varian 3900 gas chromatograph (Agilent Technologies) equipped with a flame ionization detector with splitless injection. Compounds were separated on a DB5 column (30 m × 0.25 mm i.d. × 0.25 μm thickness; Agilent Technologies) at 250°C injector temperature, and 0.5 min at 50°C, 10°C/min to 320°C, and 5 min at 320°C in the GC oven. Terpenoids were identified on the basis of their retention time and electron impact mass spectra (70 eV, *m/z* 50 to 600) after capillary GC on a HP5-MS (30 m × 0.25 mm i.d. × 0.25 μm thickness; Agilent Technologies)

with an identical oven and injector program on a PerkinElmer Clarus 680 gas chromatograph coupled to a PerkinElmer Clarus 600T mass spectrometer.

Alternatively, yeast-expressed TPS products described in Figure 5 were analyzed on an Agilent 6890N gas chromatograph equipped with an Agilent 7683 automatic liquid sampler coupled to an Agilent 5975B inert MSD. Separation was performed on a DB-Wax capillary column of 60 m × 0.32 mm i.d. × 0.50 μm film thickness (J&W Scientific). Helium was the carrier gas (flow rate of 1 mL/min), and the injector was set to 250°C in splitless mode. One microliter was injected and the GC oven temperature was programmed without initial hold time at a rate of 2.7°C/min from 70°C to 235°C (hold 10 min). The temperatures of the interface, mass spectrometry ion source, and quadrupole were 270°C, 230°C, and 150°C, respectively. The mass spectrometer was operated in electron impact ionization mode (70 eV) and the masses were scanned over a *m/z* range of 29 to 300 atomic mass units. Agilent MSD ChemStation software (G1701DA, Rev D.03.00) was used for instrument control and data processing. The mass spectra were compared with the Wiley's library reference spectral bank.

Chiral GC-MS Analysis

Chiral GC-MS analysis was conducted using an Agilent 6890 Series gas chromatograph coupled to an Agilent 5973 quadrupole mass selective detector (interface temperature, 250°C; quadrupole temperature, 150°C; source temperature, 230°C; electron energy, 70 eV). The linalool enantiomers were separated with a Rt-βDEXsm column (Restek) and He as carrier gas. The sample (1 μL) was injected without split at an initial oven temperature of 50°C. The temperature was held for 2 min and then increased to 220°C with a gradient of 3°C min⁻¹, followed by a further increase to 250°C with 60°C min⁻¹ and a hold for 3 min. Enantiomers were identified using authentic standards obtained from Sigma-Aldrich.

Separation and Structure Elucidation

Preparative GC

The enzyme assay products were separated by preparative GC using an Agilent 7890A GC instrument equipped with an HP-5 capillary column (30 m × 0.53 mm ID with 1.5 μm film) connected to a flame ionization detector (Agilent Technologies) and a preparative fraction collector with a cryostatic trap cooler (Gerstel). Glass sample traps of 1 μL volume were used. The oven was programmed as follows: initially 50°C for 1 min, then with 20°C min⁻¹ to 170°C, held for 4 min, then with 30°C min⁻¹ to 300°C, and held for 5 min to clean the column. The sample mixture (1 μL per run) was injected in splitless mode. The carrier gas was helium with a constant flow of 4.8 mL·min⁻¹. The retention time of compound 1' was 9.20 min (fraction collected from 9.17 to 9.29 min), compound 3' eluted at 9.34 min (9.29 to 9.44 min), and compound 4' [(3*R*)-3,7-dimethylocta-1,6-diene-3,5-diol] had a retention time of 9.51 min (9.44 to 9.66 min). The complete volume of the crude enzyme assay mixture was used for separation and the number of runs was adapted to the actual volume of the sample. The sample traps were subsequently eluted into HPLC vials with 90 μL CDCl₃. The extract was then transferred into 2-mm glass capillary tubes, which were fused and subjected to NMR analysis.

NMR

NMR experiments were conducted on a Bruker Avance 500 spectrometer (Bruker-Biospin) equipped with a 5 mm TCI cryoprobe (5 mm) with z-gradient operating at 500.13 MHz for ¹H and 125.76 MHz for ¹³C. Capillaries (diameter 2 mm; filling volume 85 μL CDCl₃) were used for measuring NMR spectra with standard Bruker pulse sequences. The chemical shifts of ¹H and ¹³C NMR data were referenced to the residual solvent signals (δ_H 7.24, δ_C 77.23). For compound 4', a set of experiments comprising ¹H NMR, ¹H-¹H COSY, ¹H-¹³C HSQC, ¹H-¹³C HMBC, and selective NOESY was conducted. For the latter, a mixing time of 1.5 s was

used and a Gaussian Q3 cascade tailored to the excitation width of the desired signal accomplished the selective excitation. For heteronuclear correlation experiments, coupling constants were assumed to be 145 Hz and 8 Hz for $^1J_{H-C}$ and $^nJ_{H-C}$, respectively. The structures of compound 1' [(3S)-3,7-dimethylocta-1,6-diene-3,4-diol] and compound 3' [(3R)-3,7-dimethylocta-1,6-diene-3,5-diol] were elucidated from 1H NMR and 1H - 1H COSY data. All NMR data were acquired at 298 K with a minimal relaxation delay of 2 s.

Structure Elucidation

In all GC-MS spectra of the unknown compounds, a fragment ion at m/z 152.1 indicated a linalool-derived structure. Compound 4' showed a molecular ion signal at m/z 170.1 accounting for a monohydroxylation of the parent linalool structure. 1H NMR signals at δ_H 5.93 (*dd*, 17.3/10.7 Hz, H-2), δ_H 5.22 (*dd*, 17.3/1.2 Hz, H-1a), and δ_H 5.02 (*dd*, 10.7/1.2 Hz, H-1b), together with HMBC correlations from all three proton signals to a carbon signal at δ_C 73.3 (C-3) revealed unmodified linalool-derived structure features at positions 1 to 3. The C-10 methyl group (*s*, δ_H 1.38/ δ_C 26.8) attached to C-3 showed another HMBC correlation to a methylene group at δ_C 47.2 (C-4), with corresponding 1H resonances at δ_H 1.55 (*dd*, 14.4/3.1 Hz, H-4a) and δ_H 1.78 (*dd*, 14.4/9.8 Hz, H-4b). The 1H - 1H COSY correlation from H-4 to a methine proton at δ_H 4.75 (*ddd*, 9.8/8.6/3.1 Hz, H-5), corresponding to a ^{13}C chemical shift of δ_C 66.3, revealed C-5 as the second hydroxylated position of the molecule. 1H - 1H COSY correlation from H-5 to the olefinic methine at C-6 [δ_H 5.20 (*m*, unresolved because of overlapping)/ δ_C 127.4] marked the end of the 4-membered spin system $H_2-4 \leftrightarrow H-5 \leftrightarrow H-6$. H-6 showed HMBC correlations to the quaternary carbon at δ_C 134.9 (C-7) and two methyl groups, C-8 (δ_H 1.71 (*dd*, 12.0/1.2 Hz)/ δ_C 25.7) and C-9 (δ_H 1.67 (*dd*, 12.0/1.2 Hz)/ δ_C 18.3). The topology relative to H-6 was deduced from a selective NOESY experiment. As a result, the C-8 methyl group was determined to be *cis*-positioned to H-6.

Considering the NMR data of compound 4', the structure of compound 3' was deduced from close similarities regarding chemical shifts and coupling patterns. As in compound 4', compound 3' showed a vinyl group attached to C-3, and a hydroxylated quaternary carbon that bears the C-10 methyl group (δ_H 1.28, *s*). The *exo*-methylene protons of the vinyl moiety appeared at δ_H 5.15 (*dd*, 10.7/1.5 Hz) and δ_H 5.37 (*dd*, 17.3/1.5 Hz), respectively. The corresponding methine H-2 resonated at δ_H 5.92 (*dd*, 17.3/10.7 Hz). Just as in the spectra of compound 4', a four-membered spin system $H_2-4 \leftrightarrow H-5 \leftrightarrow H-6$ was detected by 1H NMR and 1H - 1H COSY for compound 3'. The signal of H-4a appeared at δ_H 1.52 (*dd*, 14.4/2.2 Hz) and the signal of H-4b at δ_H 1.52 (*dd*, 14.4/10.8 Hz). The H-5 methine proton resonated at δ_H 4.61 (*ddd*, 10.8/8.5/2.2 Hz), again indicating hydroxylation at the corresponding carbon atom, C-5. The olefinic H-6 methine proton signal again appeared as an unresolved multiplet at δ_H 5.17. The terminal methyl groups appeared at δ_H 1.67 (C-8) and δ_H 1.63 (C-9). Because the compounds 3' and 4' are the products of an enzyme assay conducted with pure (-)-(*R*)-linalool, a configuration change at C-3 seemed unlikely. Hence, the differences in chemical shifts and coupling constants between compounds 3' and 4' reflect an opposite topology at C-5. However, because of the limited amount of substance that could be isolated and the absence of standards, the absolute configuration could not be determined. Compounds 3' and 4' represent the two diastereomers (3R, 5S) and (3R, 5R) but assignment remains to be determined.

Similar to compounds 3' and 4' described above, compound 1' also exhibits the feature of a vinyl moiety attached to the quaternary hydroxylated carbon atom C-3. The *exo*-methylene group CH_2-1 shows signals at δ_H 5.18 (*d*, 10.9) and δ_H 5.32 (*d*, 17.3 Hz), with a corresponding H-2 methine signal at δ_H 5.92 (*dd*, 17.3/10.9 Hz). The singlet signal of the C-10 methyl group appears at δ_H 1.30. The olefinic methine proton H-6 shows a multiplet signal at δ_H 5.18, which correlates in the 1H - 1H COSY spectrum with signals of the diastereotopic methylene group of CH_2-5 at δ_H 2.21 and δ_H 2.10. From this position, 1H - 1H COSY reveals a correlation with δ_H 3.44 (*dd*, 9.9/3.0 Hz) at the hydroxylated carbon atom (C-4). The methyl signals for C-8 and C-9 appear

at δ_H 1.72 (*s*) and δ_H 1.61 (*s*), respectively. As for compounds 3' and 4', the absolute configuration of compound 1' (a 4-hydroxylinalool isomer) remains to be determined.

The structure of compound 2 was readily identified as 1,2-epoxylinalool by comparison of GC retention time and mass spectrum with those of an authentic standard. However, compound 5 could not be distinguished between 9-hydroxylinalool and 8-oxo-linalool because both have the same retention time and very similar electron impact spectra (see Supplemental Figure 8 online). Compound 6 was identified as 8-hydroxylinalool by comparison of retention time and mass spectrum with a synthesized standard.

Isolation of Null Mutant Lines

Insertion mutants were selected from heterozygous SALK lines (see Supplemental Table 2 online) obtained from the Nottingham *Arabidopsis* Stock Center (Alonso et al., 2003). Two independent homozygous mutant lines were selected for each gene by genotyping, except for *TPS14* for which only one line was successfully obtained. When the rosette was formed, one young leaf was detached and used for genomic DNA extraction. The genomic DNA of three wild-type plants was used as a control. PCR genotyping was conducted using the primers provided in Supplemental Table 1 online. Loss of transcript in *null* lines was assessed using RT-PCR or qRT-PCR.

Nontargeted Analysis: UPLC-MS (Orbitrap)

Acetonitrile and formic acid of liquid chromatography-mass spectrometry grade were supplied by Thermo Fisher; water was provided by a Millipore water purification system. Analysis of leaf methanolic extracts was performed using an UHPLC system (Ultimate 3000 Dionex; Thermo Fisher Scientific) equipped with a binary pump, an online degasser, a thermostated autosampler, and a thermostatically controlled column compartment. The chromatographic separation was performed on a C18 SB column (Rapid Resolution High Density, 2.1×150 mm, 1.8 μ m particle size; Agilent Technologies) maintained at 20°C. The mobile phase consisted of water/formic acid (0.1%, v/v) (eluant A) and acetonitrile/formic acid (0.1%, v/v) (eluant B) at a flow rate of 0.25 mL/min. The gradient elution program was as follows: 0 to 1 min, 90% B; 1 to 10 min, 90% to 50% B; 10 to 16 min, 50% to 0% B; and 16 to 18 min, 0% B. The sample volume injected was 2 μ L. The liquid chromatography system was coupled to an Exactive Orbitrap mass spectrometer (Thermo Fischer Scientific) equipped with an electrospray ionization source operating in positive mode. Parameters were set at 300°C for ion transfer capillary temperature and -3700 V needle voltages. Nebulization with nitrogen sheath gas and auxiliary gas were maintained at 50 and 6 arbitrary units, respectively. The spectra were acquired within the m/z mass range of 90 to 800 atomic mass units, using a resolution of 50,000 at m/z 200 atomic mass units. The system was calibrated using lock mass, giving a mass accuracy <2 ppm. The instrument was operated using ExactiveTune software and data were processed using XcaliburQual software.

Targeted Analysis: UPLC-MS/MS Triple Quad in MRM Mode

The leaf discs or mutant open flowers were directly ground with a mortar and pestle in 5 mL methanol and incubated at 20°C for 1 h. The cleared extracts were concentrated in a stream of argon and analyzed by UPLC-MS. Analyses were performed using a Waters Quattro Premier XE equipped with an electrospray ionization source and coupled to an Acquity UPLC system (Waters USA). Chromatographic separation was achieved using an Acquity UPLC bridged ethyl hybrid C₁₈ column (100 \times 2.1 mm, 1.7 μ m; Waters) and precolumn. The mobile phase consisted of (A) water and (B) methanol, both containing 0.1% formic acid. The run started by 2 min of 95% A. Then a linear gradient was applied to reach 100% B at 12 min, followed by isocratic run using B during 2 min. Return to initial conditions was achieved in 3 min, with

a total run time of 17 min. The column was operated at 35°C with a flow rate of 0.35 mL/min, injecting 3- μ L samples. Nitrogen was used as the drying and nebulizing gas. The nebulizer gas flow was set to ~50 L/h, and the desolvation gas flow to 900 L/h. The interface temperature was set at 400°C and the source temperature at 135°C. The capillary voltage was set to 3.4 kV and the cone voltage to 25 V, the ionization was in positive or negative mode. Low mass and high mass resolution was 15 for both mass analyzers, ion energies 1 and 2 were 0.5 V, entrance and exit potential were 50 V, and detector (multiplier) gain was 650 V. Data acquisition and analysis were performed with MassLynx software (version 4.0). MRM mode (137>80.7 for linalool, 135 >106.8 for 8-hydroxylinalool, 151.2 >92.8 for 8-oxo-linalool, 167.2 >92.8 for carboxylinalool, and 153 >43.1 for 1,2-epoxylinalool) was used for quantitative analyses.

Accession Numbers

Sequence data from this article can be found in the *Arabidopsis* Genome Initiative or GenBank/EMBL databases under the following accession numbers: *TPS10* (At2g24210), *TPS14* (At1g61680), *CYP76C3* (At2g45580), *CYP71B31* (At3g53300), *SAND* (At2g28390), *TIP41* (At4g34270), *PP2A* (At1g13320), *EXP* (At4g26410), *TUB4* (At5g44340), *eGFP* (GenBank DQ768212), *mRFP* (GenBank AF506027), *TPS21* (At5g23960), *TPS24* (At3g25810), *TPS03* (At4g16740), *TPS02* (At4g16730), *TPS11* (At5g44630), *TPS23* (At3g25830), *TPS27* (At3g25820), *TPS12* (At4g13280), and *TPS13* (At4g13300).

Supplemental Data

The following materials are available in the online version of this article.

Supplemental Figure 1. Expression Heatmap of *Arabidopsis* Monoterpene Synthases and Coregulated P450s with Detailed Annotation.

Supplemental Figure 2. Confocal Microscopy Showing Colocalization of CYP76C3 and CYP71B31 with an ER Marker.

Supplemental Figure 3. Confocal Microscopy of CYP71B31:eGFP Showing ER Membranes Encircling the Chloroplasts.

Supplemental Figure 4. Characteristics and Validation of the Insertion Mutants.

Supplemental Figure 5. Linalool Emission Is Absent from Flowers of Double Mutant *tps10 tps14*.

Supplemental Figure 6. Linalool Emitted by *Arabidopsis* Flowers from the P450 Insertion Mutants.

Supplemental Figure 7. Linalool Derivatives Detected in UHPLC-Orbitrap Analysis.

Supplemental Figure 8. GC-MS Mass Spectra of the Linalool Conversion Products and References.

Supplemental Table 1. Primers Used for Genotyping of Insertion Lines, for Amplification of Open Reading Frames and 1.5-kb Promoter Region of Candidate Genes, and for qRT-PCR or RT-PCR.

Supplemental Table 2. Name and Status of Employed *Arabidopsis* Insertion Mutant Lines.

ACKNOWLEDGMENTS

The data reported in this article were generated with the support of the ANR-07-BLAN-0359 - CSD 7 grant METAMAP and of the European Community's Framework VII Program FP7/2007-2013 to the SMARTCELL project KBBE-2007-3-1-01. J.F.G. thanks the Centre National de la Recherche Scientifique and the Région Alsace for a scholarship for engineering doctorates. We thank Dr. A.J. Matich (New Zealand Plant & Food Research Limited) for the gift of reference 1,2-epoxylinalool.

AUTHOR CONTRIBUTIONS

J.F.G. prepared constructs, isolated and characterized mutants, designed experiments and performed recombinant expression, GC analyses, confocal microscopy, and wrote the first draft. R.H. and B.B. contributed to the implementation of the volatile collection system and GC-MS and UPLC-MS products analysis. F.V. and H.B. provided advice for implementation of the volatile collection system. M.M. and L.M. designed and conducted synthesis of oxygenated linalool references. M.F., F.K., and P.U. contributed to construction of yeast strains. T.G.K. determined linalool chirality. P.C. provided advice for GC analysis. R.B. contributed to the UPLC-Orbitrap analysis. J.E. supervised gene coexpression analysis and work initiation. R.L. supervised UPLC-MS/MS analyses and J.M. supervised the confocal microscopy. C.P. and F.B. conducted GC purification. C.P. and B.S. elucidated the structures of P450 products by NMR. D.W.R., B.S., and J.G. supervised work and article preparation.

Received August 22, 2013; revised October 16, 2013; accepted November 5, 2013; published November 27, 2013.

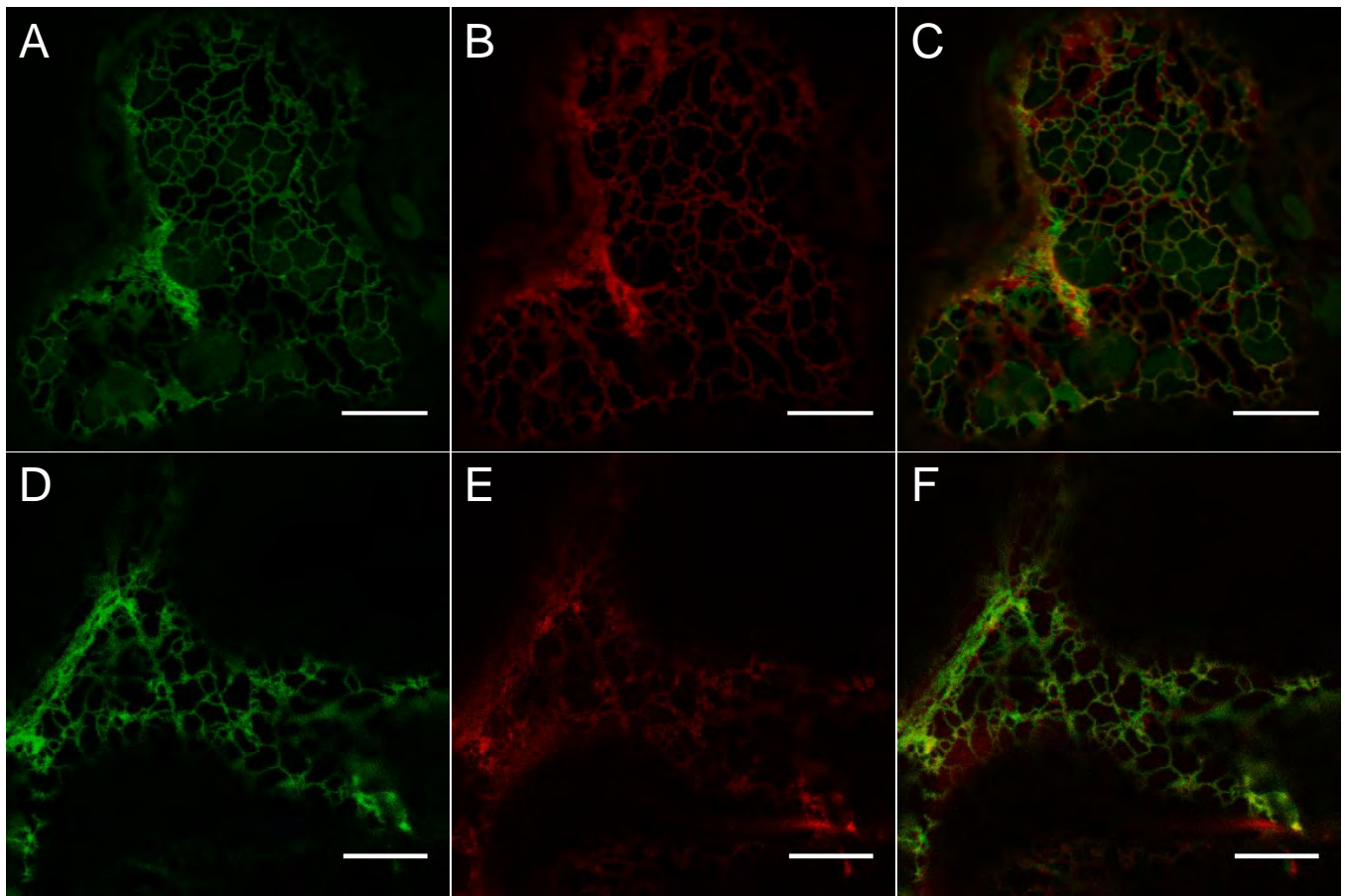
REFERENCES

- Aharoni, A., Giri, A.P., Deuerlein, S., Griepink, F., de Kogel, W.J., Verstappen, F.W., Verhoeven, H.A., Jongsma, M.A., Schwab, W., and Bouwmeester, H.J. (2003). Terpenoid metabolism in wild-type and transgenic *Arabidopsis* plants. *Plant Cell* **15**: 2866–2884.
- Aharoni, A., Giri, A.P., Verstappen, F.W., Berteaux, C.M., Sevenier, R., Sun, Z., Jongsma, M.A., Schwab, W., and Bouwmeester, H.J. (2004). Gain and loss of fruit flavor compounds produced by wild and cultivated strawberry species. *Plant Cell* **16**: 3110–3131.
- Alonso, J.M., et al. (2003). Genome-wide insertional mutagenesis of *Arabidopsis thaliana*. *Science* **301**: 653–657.
- Andersson, M.X., Goksör, M., and Sandelius, A.S. (2007). Optical manipulation reveals strong attracting forces at membrane contact sites between endoplasmic reticulum and chloroplasts. *J. Biol. Chem.* **282**: 1170–1174.
- Aubourg, S., Lecharny, A., and Bohlmann, J. (2002). Genomic analysis of the terpenoid synthase (AtTPS) gene family of *Arabidopsis thaliana*. *Mol. Genet. Genomics* **267**: 730–745.
- Austin, J.R., II, Frost, E., Vidi, P.-A., Kessler, F., and Staehelin, L.A. (2006). Plastoglobules are lipoprotein subcompartments of the chloroplast that are permanently coupled to thylakoid membranes and contain biosynthetic enzymes. *Plant Cell* **18**: 1693–1703.
- Bak, S., Beisson, F., Bishop, G., Hamberger, B., Höfer, R., Paquette, S., and Werck-Reichhart, D. (2011). Cytochromes P450. In *The Arabidopsis Book* **9**: e0144, doi/.
- Berteaux, C.M., Schalk, M., Karp, F., Maffei, M., and Croteau, R. (2001). Demonstration that menthofuran synthase of mint (*Mentha*) is a cytochrome P450 monooxygenase: Cloning, functional expression, and characterization of the responsible gene. *Arch. Biochem. Biophys.* **390**: 279–286.
- Bohlmann, J., Martin, D., Oldham, N.J., and Gershenzon, J. (2000). Terpenoid secondary metabolism in *Arabidopsis thaliana*: cDNA cloning, characterization, and functional expression of a myrcene/(E)-beta-ocimene synthase. *Arch. Biochem. Biophys.* **375**: 261–269.
- Boulaflous, A., Saint-Jore-Dupas, C., Herranz-Gordo, M.C., Pagny-Salehabadi, S., Plasson, C., Garidou, F., Kiefer-Meyer, M.C., Ritzenthaler, C., Faye, L., and Gomord, V. (2009). Cytosolic N-terminal arginine-based signals together with a luminal signal target a type II membrane protein to the plant ER. *BMC Plant Biol.* **9**: 144.
- Bréhélin, C., and Kessler, F. (2008). The plastoglobule: A bag full of lipid biochemistry tricks. *Photochem. Photobiol.* **84**: 1388–1394.

- Breuers, F.K., Bräutigam, A., Geimer, S., Welzel, U.Y., Stefano, G., Renna, L., Brandizzi, F., and Weber, A.P. (2012). Dynamic remodeling of the plastid envelope membranes - A tool for chloroplast envelope in vivo localizations. *Front Plant Sci* **3**: 7.
- Campbell, R.E., Tour, O., Palmer, A.E., Steinbach, P.A., Baird, G.S., Zacharias, D.A., and Tsien, R.Y. (2002). A monomeric red fluorescent protein. *Proc. Natl. Acad. Sci. USA* **99**: 7877–7882.
- Chen, F., Tholl, D., D'Auria, J.C., Farooq, A., Pichersky, E., and Gershenzon, J. (2003). Biosynthesis and emission of terpenoid volatiles from *Arabidopsis* flowers. *Plant Cell* **15**: 481–494.
- Clough, S.J., and Bent, A.F. (1998). Floral dip: A simplified method for *Agrobacterium*-mediated transformation of *Arabidopsis thaliana*. *Plant J.* **16**: 735–743.
- Collu, G., Unver, N., Peltenburg-Looman, A.M., van der Heijden, R., Verpoorte, R., and Memelink, J. (2001). Geraniol 10-hydroxylase, a cytochrome P450 enzyme involved in terpenoid indole alkaloid biosynthesis. *FEBS Lett.* **508**: 215–220.
- Czechowski, T., Stitt, M., Altmann, T., Udvardi, M.K., and Scheible, W.R. (2005). Genome-wide identification and testing of superior reference genes for transcript normalization in *Arabidopsis*. *Plant Physiol.* **139**: 5–17.
- Ehltling, J., Sauveplane, V., Olry, A., Ginglinger, J.F., Provart, N.J., and Werck-Reichhart, D. (2008). An extensive (co-)expression analysis tool for the cytochrome P450 superfamily in *Arabidopsis thaliana*. *BMC Plant Biol.* **8**: 47.
- Emanuelsson, O., Nielsen, H., and von Heijne, G. (1999). ChloroP, a neural network-based method for predicting chloroplast transit peptides and their cleavage sites. *Protein Sci.* **8**: 978–984.
- Emanuelsson, O., Nielsen, H., Brunak, S., and von Heijne, G. (2000). Predicting subcellular localization of proteins based on their N-terminal amino acid sequence. *J. Mol. Biol.* **300**: 1005–1016.
- Erdogan, A., and Ozkan, A. (2013). A comparative study of cytotoxic, membrane and DNA damaging effects of *Origanum majorana*'s essential oil and its oxygenated monoterpene component linalool on parental and epirubicin-resistant H1299 cells. *Biologia* **68**: 754–761.
- Fäldt, J., Arimura, G., Gershenzon, J., Takabayashi, J., and Bohlmann, J. (2003). Functional identification of AtTPS03 as (*E*)-beta-ocimene synthase: A monoterpene synthase catalyzing jasmonate- and wound-induced volatile formation in *Arabidopsis thaliana*. *Planta* **216**: 745–751.
- Field, B., and Osbourn, A.E. (2008). Metabolic diversification— independent assembly of operon-like gene clusters in different plants. *Science* **320**: 543–547.
- Field, B., Fiston-Lavier, A.S., Kemen, A., Geisler, K., Quesneville, H., and Osbourn, A.E. (2011). Formation of plant metabolic gene clusters within dynamic chromosomal regions. *Proc. Natl. Acad. Sci. USA* **108**: 16116–16121.
- Fischer, M.J., Meyer, S., Claudel, P., Bergdoll, M., and Karst, F. (2011). Metabolic engineering of monoterpene synthesis in yeast. *Biotechnol. Bioeng.* **108**: 1883–1892.
- Fischer, M.J.C., Meyer, S., Claudel, P., Perrin, M., Ginglinger, J.F., Gertz, C., Masson, J.E., Werck-Reinhardt, D., Hugueney, P., and Karst, F. (2013). Specificity of *Ocimum basilicum* geraniol synthase modified by its expression in different heterologous systems. *J. Biotechnol.* **163**: 24–29.
- Francis, M.J.O., and Allcock, C. (1969). Geraniol β -d-glucoside; occurrence and synthesis in rose flowers. *Phytochemistry* **8**: 1339–1347.
- Franke, R., Humphreys, J.M., Hemm, M.R., Denault, J.W., Ruegger, M.O., Cusumano, J.C., and Chapple, C. (2002). The *Arabidopsis* REF8 gene encodes the 3-hydroxylase of phenylpropanoid metabolism. *Plant J.* **30**: 33–45.
- Froehlich, J.E., Itoh, A., and Howe, G.A. (2001). Tomato allene oxide synthase and fatty acid hydroperoxide lyase, two cytochrome P450s involved in oxylipin metabolism, are targeted to different membranes of chloroplast envelope. *Plant Physiol.* **125**: 306–317.
- Gavira, C., Höfer, R., Lesot, A., Lambert, F., Zucca, J., and Werck-Reichhart, D. (2013). Challenges and pitfalls of P450-dependent (+)-valencene bioconversion by *Saccharomyces cerevisiae*. *Metab. Eng.* **18**: 25–35.
- Geu-Flores, F., Nour-Eldin, H.H., Nielsen, M.T., and Halkier, B.A. (2007). USER fusion: A rapid and efficient method for simultaneous fusion and cloning of multiple PCR products. *Nucleic Acids Res.* **35**: e55.
- Gietz, R.D., and Schiestl, R.H. (2007). High-efficiency yeast transformation using the LiAc/SS carrier DNA/PEG method. *Nat. Protoc.* **2**: 31–34.
- Hallahan, D.L., Lau, S.M.C., Harder, P.A., Smiley, D.W., Dawson, G.W., Pickett, J.A., Christoffersen, R.E., and O'Keefe, D.P. (1994). Cytochrome P-450-catalysed monoterpene oxidation in catmint (*Nepeta racemosa*) and avocado (*Persea americana*); evidence for related enzymes with different activities. *Biochim. Biophys. Acta.* **1201**: 94–100.
- Hallahan, D.L., Nugent, J.H.A., Hallahan, B.J., Dawson, G.W., Smiley, D.W., West, J.M., and Wallsgrove, R.M. (1992). Interaction of avocado (*Persea americana*) cytochrome-P-450 with monoterpenoids. *Plant Physiol.* **98**: 1290–1297.
- Hamberger, B., and Bak, S. (2013). Plant P450s as versatile drivers for evolution of species-specific chemical diversity. *Philos. Trans. R. Soc. Lond. B. Biol. Sci.* **368**: 20120426.
- Haudenschild, C., Schalk, M., Karp, F., and Croteau, R. (2000). Functional expression of regiospecific cytochrome P450 limonene hydroxylases from mint (*Mentha* spp.) in *Escherichia coli* and *saccharomyces cerevisiae*. *Arch. Biochem. Biophys.* **379**: 127–136.
- Heitz, T., Widemann, E., Lugan, R., Miesch, L., Ullmann, P., Désaubry, L., Holder, E., Grausem, B., Kandel, S., Miesch, M., Werck-Reichhart, D., and Pinot, F. (2012). Cytochromes P450 CYP94C1 and CYP94B3 catalyze two successive oxidation steps of plant hormone Jasmonoyl-isoleucine for catabolic turnover. *J. Biol. Chem.* **287**: 6296–6306.
- Helliwell, C.A., Sullivan, J.A., Mould, R.M., Gray, J.C., Peacock, W.J., and Dennis, E.S. (2001). A plastid envelope location of *Arabidopsis* ent-kaurene oxidase links the plastid and endoplasmic reticulum steps of the gibberellin biosynthesis pathway. *Plant J.* **28**: 201–208.
- Herken, E.N., Celik, A., Aslan, M., and Aydinlik, N. (2012). The constituents of essential oil: Antimicrobial and antioxidant activity of *Micromeria congesta* Boiss. & Hausskn. ex Boiss. from East Anatolia. *J. Med. Food* **15**: 835–839.
- Höfer, R., Dong, L., André, F., Ginglinger, J.F., Lugan, R., Gavira, C., Grec, S., Lang, G., Memelink, J., Van Der Krol, S., Bouwmeester, H., and Werck-Reichhart, D. (2013). Geraniol hydroxylase and hydroxygeraniol oxidase activities of the CYP76 family of cytochrome P450 enzymes and potential for engineering the early steps of the (seco) iridoid pathway. *Metab. Eng.* **20**: 221–232.
- Hoffmann, M.H., Bremer, M., Schneider, K., Burger, F., Stolle, E., and Moritz, G. (2003). Flower visitors in a natural population of *Arabidopsis thaliana*. *Plant Biol.* **5**: 491–494.
- Huang, M., Abel, C., Sohrabi, R., Petri, J., Haupt, I., Cosimano, J., Gershenzon, J., and Tholl, D. (2010). Variation of herbivore-induced volatile terpenes among *Arabidopsis* ecotypes depends on allelic differences and subcellular targeting of two terpene synthases, TPS02 and TPS03. *Plant Physiol.* **153**: 1293–1310.

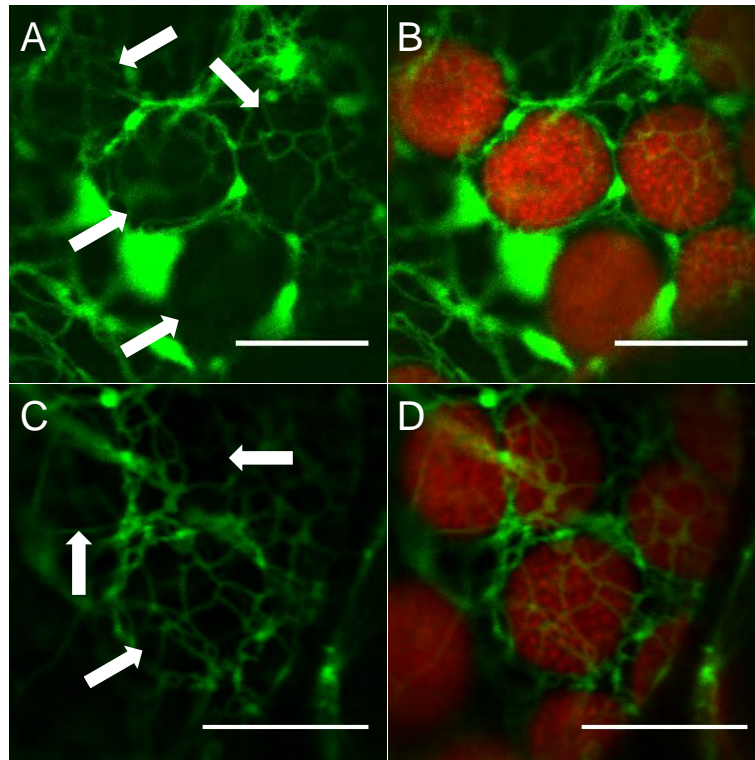
- Huang, M., Sanchez-Moreiras, A.M., Abel, C., Sohrabi, R., Lee, S., Gershenzon, J., and Tholl, D. (2012). The major volatile organic compound emitted from *Arabidopsis thaliana* flowers, the sesquiterpene (E)- β -caryophyllene, is a defense against a bacterial pathogen. *New Phytol.* **193**: 997–1008.
- Jefferson, R.A., Kavanagh, T.A., and Bevan, M.W. (1987). GUS fusions: Beta-glucuronidase as a sensitive and versatile gene fusion marker in higher plants. *EMBO J.* **6**: 3901–3907.
- Jerković, I., and Marijanović, Z. (2010). Oak (*Quercus frainetto* Ten.) honeydew honey—approach to screening of volatile organic composition and antioxidant capacity (DPPH and FRAP assay). *Molecules* **15**: 3744–3756.
- Karp, F., Mihaliak, C.A., Harris, J.L., and Croteau, R. (1990). Monoterpene biosynthesis: Specificity of the hydroxylations of (-)-limonene by enzyme preparations from peppermint (*Mentha piperita*), spearmint (*Mentha spicata*), and perilla (*Perilla frutescens*) leaves. *Arch. Biochem. Biophys.* **276**: 219–226.
- Kim, J., and DellaPenna, D. (2006). Defining the primary route for lutein synthesis in plants: The role of *Arabidopsis* carotenoid beta-ring hydroxylase CYP97A3. *Proc. Natl. Acad. Sci. USA* **103**: 3474–3479.
- Knudsen, J.T., Eriksson, R., Gershenzon, J., and Stahl, B. (2006). Diversity and distribution of floral scent. *Bot. Rev.* **72**: 1–120.
- Kreck, M., Püschel, S., Wüst, M., and Mosandl, A. (2003). Biogenetic studies in *Syringa vulgaris* L.: Synthesis and bioconversion of deuterium-labeled precursors into lilac aldehydes and lilac alcohols. *J. Agric. Food Chem.* **51**: 463–469.
- Lee, S., and Chappell, J. (2008). Biochemical and genomic characterization of terpene synthases in *Magnolia grandiflora*. *Plant Physiol.* **147**: 1017–1033.
- Lee, S., Badiyan, S., Bevan, D.R., Herde, M., Gatz, C., and Tholl, D. (2010). Herbivore-induced and floral homoterpene volatiles are biosynthesized by a single P450 enzyme (CYP82G1) in *Arabidopsis*. *Proc. Natl. Acad. Sci. USA* **107**: 21205–21210.
- Lupien, S., Karp, F., Wildung, M., and Croteau, R. (1999). Regiospecific cytochrome P450 limonene hydroxylases from mint (*Mentha*) species: cDNA isolation, characterization, and functional expression of (-)-4S-limonene-3-hydroxylase and (-)-4S-limonene-6-hydroxylase. *Arch. Biochem. Biophys.* **368**: 181–192.
- Maietti, S., Rossi, D., Guerrini, A., Useli, C., Romagnoli, C., Poli, F., Bruni, R., and Sacchetti, G. (2013). A multivariate analysis approach to the study of chemical and functional properties of chemo-diverse plant derivatives: Lavender essential oils. *Flavour Frag. J.* **28**: 144–154.
- Mathur, J., Mammone, A., and Barton, K.A. (2012). Organelle extensions in plant cells. *J. Integr. Plant Biol.* **54**: 851–867.
- Match, A.J., Comeskey, D.J., Bunn, B.J., Hunt, M.B., and Rowan, D.D. (2011). Biosynthesis and enantioselectivity in the production of the lilac compounds in *Actinidia arguta* flowers. *Phytochemistry* **72**: 579–586.
- Matsuno, M., et al. (2009). Evolution of a novel phenolic pathway for pollen development. *Science* **325**: 1688–1692.
- Mehrshahi, P., Stefano, G., Andaloro, J.M., Brandizzi, F., Froehlich, J.E., and DellaPenna, D. (2013). Transorganellar complementation redefines the biochemical continuity of endoplasmic reticulum and chloroplasts. *Proc. Natl. Acad. Sci. USA* **110**: 12126–12131.
- Nagegowda, D.A., Gutensohn, M., Wilkerson, C.G., and Dudareva, N. (2008). Two nearly identical terpene synthases catalyze the formation of nerolidol and linalool in snapdragon flowers. *Plant J.* **55**: 224–239.
- Nelson, D., and Werck-Reichhart, D. (2011). A P450-centric view of plant evolution. *Plant J.* **66**: 194–211.
- Nour-Eldin, H.H., Hansen, B.G., Nørholm, M.H., Jensen, J.K., and Halkier, B.A. (2006). Advancing uracil-excision based cloning towards an ideal technique for cloning PCR fragments. *Nucleic Acids Res.* **34**: e122.
- Omura, T., and Sato, R. (1964). Carbon monoxide-binding pigment of liver microsomes. I. Evidence for its hemoprotein nature. *J. Biol. Chem.* **239**: 2370–2378.
- Pellmyr, O., Thien, L.B., Bergström, G., and Groth, I. (1990). Pollination of new caledonian winteraceae - opportunistic shifts or parallel radiation with their pollinators. *Plant Syst. Evol.* **173**: 143–157.
- Pfaffl, M.W. (2001). A new mathematical model for relative quantification in real-time RT-PCR. *Nucleic Acids Res.* **29**: e45.
- Pichersky, E., Raguso, R.A., Lewinsohn, E., and Croteau, R. (1994). Floral scent production in *Clarkia* (Onagraceae). 1. Localization and developmental modulation of monoterpene emission and linalool synthase activity. *Plant Physiol.* **106**: 1533–1540.
- Raguso, R.A., and Pichersky, E. (1999). New Perspectives in Pollination Biology: Floral Fragrances. A day in the life of a linalool molecule: Chemical communication in a plant-pollinator system. Part 1: Linalool biosynthesis in flowering plants. *Plant Species Biol.* **14**: 95–120.
- Ro, D.K., Ehltling, J., Keeling, C.I., Lin, R., Mattheus, N., and Bohlmann, J. (2006). Microarray expression profiling and functional characterization of AtTPS genes: Duplicated *Arabidopsis thaliana* sesquiterpene synthase genes At4g13280 and At4g13300 encode root-specific and wound-inducible (Z)-gamma-bisabolene synthases. *Arch. Biochem. Biophys.* **448**: 104–116.
- Rohloff, J., and Bones, A.M. (2005). Volatile profiling of *Arabidopsis thaliana* - putative olfactory compounds in plant communication. *Phytochemistry* **66**: 1941–1955.
- Sagt, C.M.J., et al (2009). Peroxirection: A novel secretion pathway in the eukaryotic cell. *BMC Biotechnol.* **9**: 48.
- Sauveplane, V., Kandel, S., Kastner, P.-E., Ehltling, J., Compagnon, V., Werck-Reichhart, D., and Pinot, F. (2009). *Arabidopsis thaliana* CYP77A4 is the first cytochrome P450 able to catalyze the epoxidation of free fatty acids in plants. *FEBS J.* **276**: 719–735.
- Schlaman, H.R.M., Risseuw, E., Franke-van Dijk, M.E.I., and Hooykaas, P.J.J. (1994). Nucleotide sequence corrections of the *uidA* open reading frame encoding beta-glucuronidase. *Gene* **138**: 259–260.
- Schoch, G., Goepfert, S., Morant, M., Hehn, A., Meyer, D., Ullmann, P., and Werck-Reichhart, D. (2001). CYP98A3 from *Arabidopsis thaliana* is a 3'-hydroxylase of phenolic esters, a missing link in the phenylpropanoid pathway. *J. Biol. Chem.* **276**: 36566–36574.
- Schuler, M.A., Duan, H., Bilgin, M., and Ali, S. (2006). *Arabidopsis* cytochrome P450s through the looking glass: A window on plant biochemistry. *Phytochem. Rev.* **5**: 205–237.
- Sharma, M.L., and Chand, T. (1996). Allylic oxidation in terpenoids: Synthesis of (\pm)-E-linalool-1-oic acid, (\pm)-E-9-hydroxylinalool and (\pm)-7-hydroxyterpineol. *Proc. Indian Acad. Sci. Chem. Sci.* **108**: 21–26.
- Singh, A., Sharma, M.L., and Singh, J. (2009). Synthesis of (\pm)- (E)-2,6-dimethyl-6-hydroxy-2,7-octadienoic acid, its methyl ester and (\pm)- (E)-2,6-dimethyl-octa-2,7-diene-1,6-diol over solid support using microwave. *Indian J. Chem., Sect. B: Org. Chem. Incl. Med. Chem.* **48**: 452–454.
- Small, I., Peeters, N., Legeai, F., and Lurin, C. (2004). Predotar: A tool for rapidly screening proteomes for N-terminal targeting sequences. *Proteomics* **4**: 1581–1590.
- Steeghs, M., Bais, H.P., de Gouw, J., Goldan, P., Kuster, W., Northway, M., Fall, R., and Vivanco, J.M. (2004). Proton-transfer-reaction mass spectrometry as a new tool for real time analysis of root-secreted volatile organic compounds in *Arabidopsis*. *Plant Physiol.* **135**: 47–58.
- Terry, I., Moore, C.J., Walter, G.H., Forster, P.I., Roemer, R.B., Donaldson, J.D., and Machin, P.J. (2004). Association of cone thermogenesis and volatiles with pollinator specificity in *Macrozamia cycads*. *Plant Syst. Evol.* **243**: 233–247.

- Tholl, D., and Lee, S.** (2011). Terpene specialized metabolism in *Arabidopsis thaliana*. In *The Arabidopsis Book* **9**: e0143, doi/.
- Tholl, D., Chen, F., Petri, J., Gershenzon, J., and Pichersky, E.** (2005). Two sesquiterpene synthases are responsible for the complex mixture of sesquiterpenes emitted from *Arabidopsis* flowers. *Plant J.* **42**: 757–771.
- Tian, L., Musetti, V., Kim, J., Magallanes-Lundback, M., and DellaPenna, D.** (2004). The *Arabidopsis* LUT1 locus encodes a member of the cytochrome p450 family that is required for carotenoid epsilon-ring hydroxylation activity. *Proc. Natl. Acad. Sci. USA* **101**: 402–407.
- Voinnet, O., Rivas, S., Mestre, P., and Baulcombe, D.** (2003). An enhanced transient expression system in plants based on suppression of gene silencing by the p19 protein of tomato bushy stunt virus. *Plant J.* **33**: 949–956.
- Watanabe, N., Nakajima, R., Watanabe, S., Moon, J.H., Inagaki, J., Sakata, K., Yagi, A., and Ina, K.** (1994). Linalyl and bornyl disaccharide glycosides from *Gardenia jasminoides* flowers. *Phytochemistry* **37**: 457–459.
- Watson, C.J.W., Froehlich, J.E., Josefsson, C.A., Chapple, C., Durst, F., Benveniste, I., and Coolbaugh, R.C.** (2001). Localization of CYP86B1 in the outer envelope of chloroplasts. *Plant Cell Physiol.* **42**: 873–878.
- Wilkins, A.L., Lu, Y., and Tan, S.T.** (1993). Extractives from New Zealand honeys. 4. Linalool derivatives and other components from nodding thistle (*Carduus Nutans*) honey. *J. Agric. Food Chem.* **41**: 873–878.



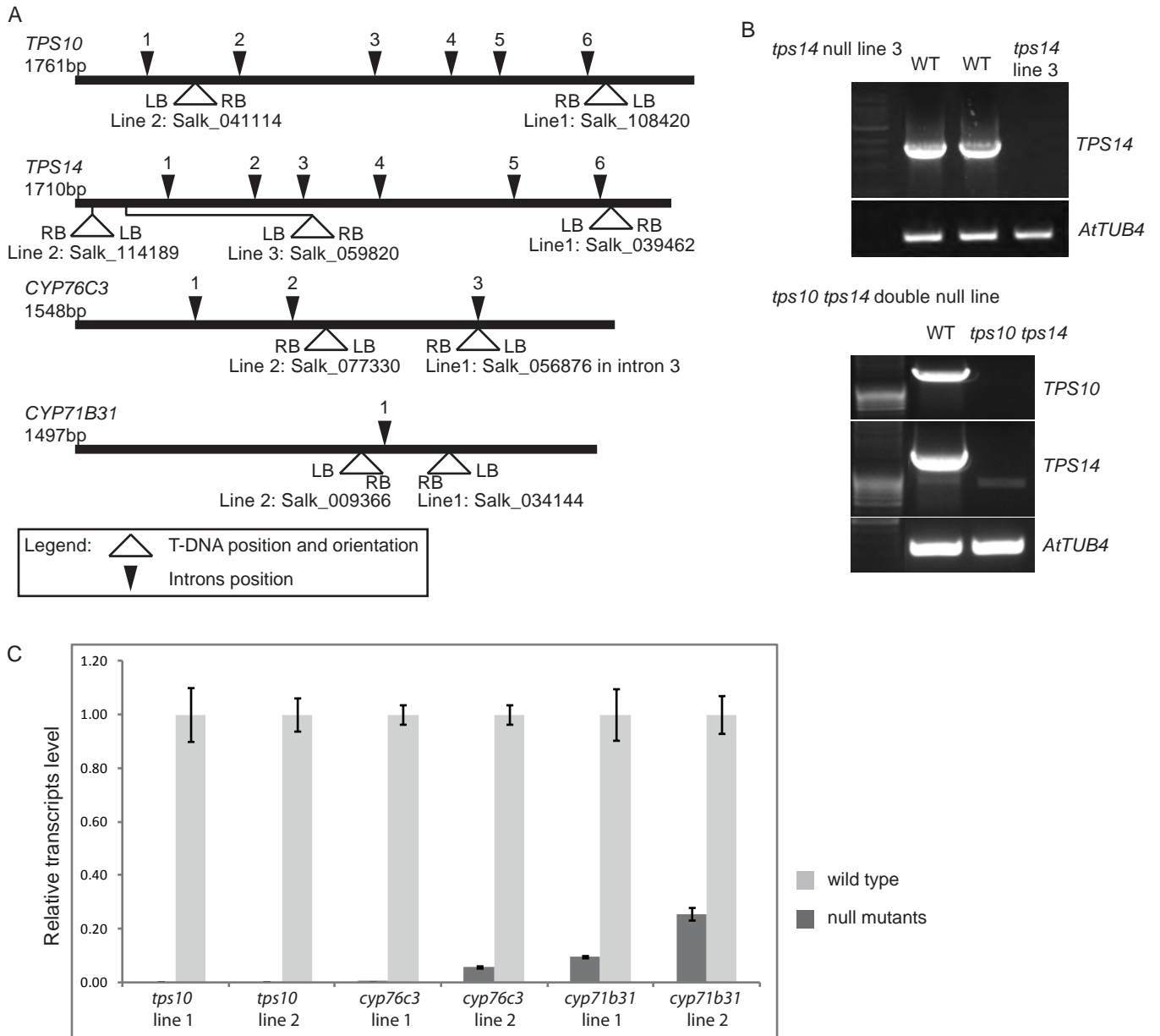
Supplemental Figure 2: Confocal microscopy showing co-localization of CYP76C3 and CYP71B31 with an ER marker.

CYP76C3:eGFP and CYP71B31:eGFP ER were transiently expressed in *N. benthamiana* epidermal cells together with the ER marker mRFP:HDEL and visualized by confocal microscopy. (A) CYP76C3:eGFP, (D) CYP71B31:eGFP, (B and E) mRFP:HDEL, (C and F) merged. Scale bar: 10 μ m.



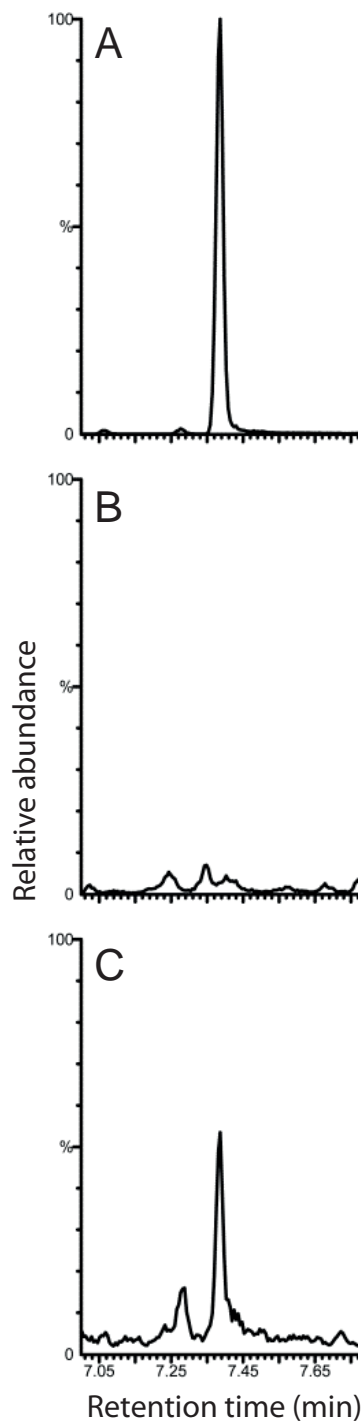
Supplemental Figure 3: Confocal microscopy of CYP71B31:eGFP showing ER membranes encircling the chloroplasts.

Chloroplasts (chlorophyll autofluorescence in plastids stroma) in red. (A and C) CYP71B31:eGFP localized on ER membranes. (B and D) merged with chloroplast autofluorescence. Scale bar: 10 μm . Arrows (A and C) point to cavities formed by ER in which chloroplasts fit perfectly with region of potential contact between ER and plastid envelope (B and D).



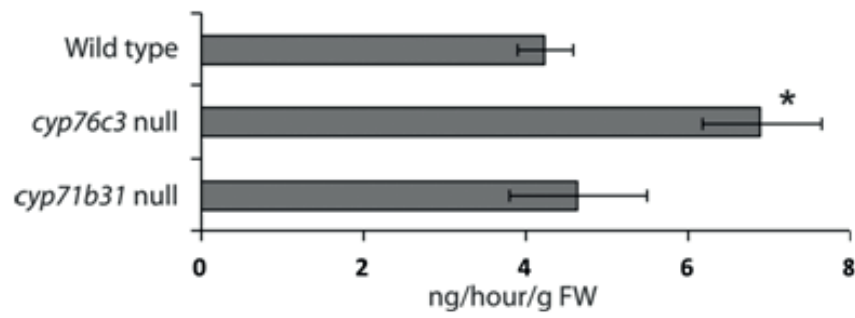
Supplemental Figure 4: Characteristics and validation of the insertion mutants.

(A) Positions of T-DNA in candidate genes for each insertion line tested. (B) RT-PCR on transcripts for insertion mutants *tps14* line 3 and double mutant line *tps10 tps14*. (C) Transcript levels in flowers measured by qRT-PCR for insertion mutants *tps10* lines 1 and 2, *cyp76c3* lines 1 and 2, and *cyp71b31* lines 1 and 2. The T-DNA was not located in TPS14 insertion lines 1 and 2.



Supplemental Figure 5: Linalool emission is absent from flowers of double mutant *tps10 tps14*.

The emitted volatiles of flower bouquets (~60 inflorescences) of wild type and double mutant line *tps10 tps14* were collected for 6 hours and analyzed in GC-MS as described in Methods. (A) Linalool reference, (B) double mutant *tps10 tps14*, (C) wild type. Linalool emission was not affected in single mutant lines *tps10* and *tps14* (data not shown).



Supplemental Figure 6: Linalool emitted by *Arabidopsis* flowers from the P450 insertion mutants.

A small but significant increase of linalool emission is observed with the flowers of *cyp76c3* insertion line. Error bars: SE, n=3. *, $p < 0.05$.

References	RT (min)	Mass	Detected masses			Additional substructures detected							
			[M+H] ⁺	[M+H-H ₂ O] ⁺	[M+H-2H ₂ O] ⁺	mass 1	formula 1	mass 2	formula 2	mass 3	formula 3	mass 4	formula 4
linalool	14.02	154.1352	155.1431	137.1326		153.1275	C10H17O	135.1169	C10H15	123.1170	C9H15	107.0858	C8H11
1,2 epoxy-linalool	11.84	170.1301	171.1380	153.1275	135.1169	123.1170	C9H15	95.0859	C7H11				
8-hydroxylinalool	8.05	170.1301		153.1274	135.1169	109.1015	C8H13	107.0858	C8H11	93.0702	C7H9		
8-oxo-linalool	9.67	168.1145		151.1118	133.1013	123.1170	C9H15	107.0858	C8H11	95.0859	C7H11	93.0702	C7H9
lilac alcohol	10.32	170.1301	171.1380		135.1169	123.1170	C9H15						
lilac alcohol epoxide	7.18	186.1250	187.1329	169.1224	151.1118	123.1170	C9H15						

Compound 1 - RT: 4.52 min			Detected masses			Compound 2 - RT: 6.38 min			Detected masses		
Possible structure	Brut formula	Mass	[M+H] ⁺	[M+H-H ₂ O] ⁺	[M+H-2H ₂ O] ⁺	Possible structure	Brut formula	Mass	[M+H] ⁺	[M+H-H ₂ O] ⁺	[M+H-2H ₂ O] ⁺
8-carboxy-dihydro-linalool	C10H18O3	186.1250		169.1224	151.1118	hydroxy-linalool	C10H18O2	170.1301		153.1275	
6-hydroxy-8-oxo-linalool						lilac alcohol					
epoxy-hydroxy-linalool						1,2- or 6,7- epoxy-linalool					
epoxy-linalool oxide						linalool oxide					
epoxy-8-oxo-dihydro-linalool						8-oxo-dihydro-linalool					
+ hexose (+C6H12O6 - H2O)	C16H28O8	348.1778	349.1858	331.1751		+ hexose (+C6H12O6 - H2O)	C16H28O7	332.1830	333.1908	315.1802	
Additional substructure detected						Additional substructure detected					
	C9H14	122.1090	123.1170				C7H8	92.0621	93.0702		
	C10H12	132.0934	133.1012				C7H10	94.0777	95.0859		
							C8H10	106.0777	107.0858		

Compound 3 - RT: 7.40 min			Detected masses			Compound 4 - RT: 7.44 min			Detected masses		
Possible structure	Brut formula	Mass	[M+H] ⁺	[M+H-H ₂ O] ⁺	[M+H-2H ₂ O] ⁺	Possible structure	Brut formula	Mass	[M+H] ⁺	[M+H-H ₂ O] ⁺	[M+H-2H ₂ O] ⁺
hydroxy-linalool	C10H18O2	170.1301		153.1275	135.1169	hydroxy-linalool	C10H18O2	170.1301	171.1380		
1,2- or 6,7- epoxy-linalool						lilac alcohol					
linalool oxide						linalool oxide					
8-oxo-dihydro-linalool						8-oxo-dihydro-linalool					
+ malonyl hexose (+C9H16O10 - 2H2O)	C19H30O10	418.1833		401.1806		+ hexose (+C6H12O6 - H2O)	C16H28O7	332.1830	333.1908		
Additional substructure detected						malonyl glucose-H2O	C9H12O8	248.0525	249.0605		

Compound 5 - RT: 7.56 min			Detected masses			Compound 6 - RT: 7.60 min			Detected masses		
Possible structure	Brut formula	Mass	[M+H] ⁺	[M+H-H ₂ O] ⁺	[M+H-2H ₂ O] ⁺	Possible structure	Brut formula	Mass	[M+H] ⁺	[M+H-H ₂ O] ⁺	[M+H-2H ₂ O] ⁺
hydroxy-linalool	C10H18O2	170.1301	171.1380	153.1275		8-carboxy-linalool	C10H16O3	184.1094	185.1173	167.1067	
lilac alcohol						hydroxy-oxo-linalool					
linalool oxide						epoxy-lilac aldehyde					
8-oxo-dihydro-linalool						epoxy-8-oxo-linalool					
+ hexose (+C6H12O6 - H2O)	C16H28O7	332.1828	333.1908								

Compound 7 - RT: 7.67 min			Detected masses			Compound 8 - RT: 7.92 min			Detected masses		
Possible structure	Brut formula	Mass	[M+H] ⁺	[M+H-H ₂ O] ⁺	[M+H-2H ₂ O] ⁺	Possible structure	Brut formula	Mass	[M+H] ⁺	[M+H-H ₂ O] ⁺	[M+H-2H ₂ O] ⁺
hydroxy-linalool	C10H18O2	170.1301	171.1379	153.1275	135.1169	linalool	C10H18O	154.1352	155.1431		
1,2- or 6,7- epoxy-linalool						+ malonyl hexose (+C9H16O10 - 2H2O)	C19H30O9	402.1884	403.1962	385.1856	
linalool oxide						hydroxy-dihydro-linalool	C10H20O2	172.1461		155.1431	
8-oxo-dihydro-linalool						1,2- or 6,7-epoxy-dihydro-linalool					
+ malonyl hexose (+C9H16O10 - 2H2O)	C19H30O10	418.1833	419.1912	401.1806		+ malonyl hexose (+C9H16O10 - 2H2O)	C19H32O10	420.1993	403.1962	385.1856	
Additional substructure detected						Additional substructure detected					
malonyl glucose-H2O	C9H12O8	248.0525	249.0605			malonyl glucose-H2O	C9H12O8	248.0525	249.0605		

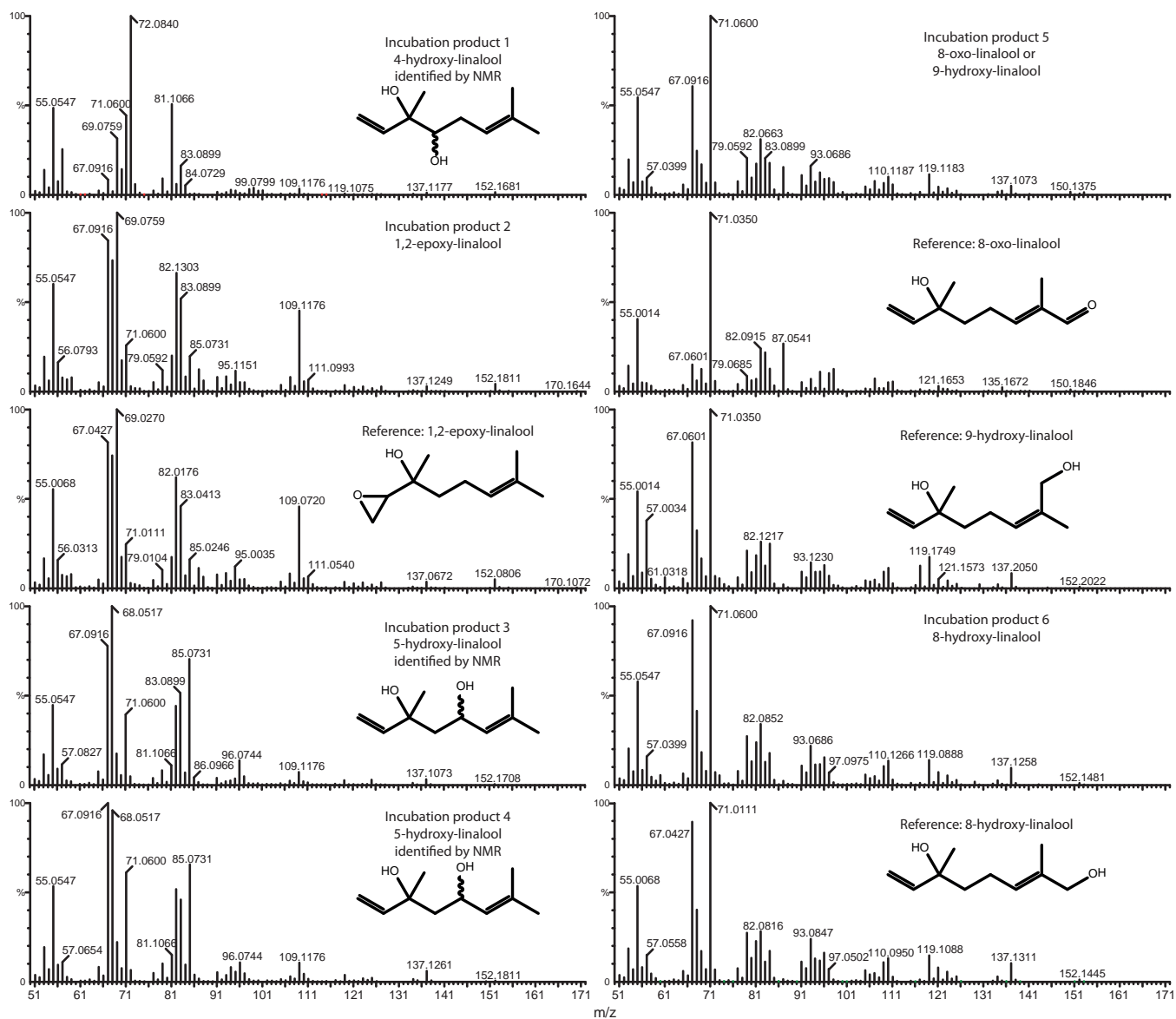
Compound 9 - RT: 8.48 min			Detected masses			Compound 10 - RT: 8.60 min			Detected masses		
Possible structure	Brut formula	Mass	[M+H] ⁺	[M+H-H ₂ O] ⁺	[M+H-2H ₂ O] ⁺	Possible structure	Brut formula	Mass	[M+H] ⁺	[M+H-H ₂ O] ⁺	[M+H-2H ₂ O] ⁺
hydroxy-linalool	C10H18O2	170.1301	171.1380			hydroxy-dihydro-linalool	C10H20O2	172.1461		155.1431	137.1326
lilac alcohol						1,2- or 6,7-epoxy-dihydro-linalool					
linalool oxide						Additional substructure detected					
8-oxo-dihydro-linalool							C7H10	94.0777	95.0859		
+ malonyl hexose (+C9H16O10 - 2H2O)	C19H30O10	418.1833	419.1911	401.1806							

Compound 11 - RT: 8.62 min			Detected masses			Compound 12 - RT: 8.85 min			Detected masses		
Possible structure	Brut formula	Mass	[M+H] ⁺	[M+H-H ₂ O] ⁺	[M+H-2H ₂ O] ⁺	Possible structure	Brut formula	Mass	[M+H] ⁺	[M+H-H ₂ O] ⁺	[M+H-2H ₂ O] ⁺
hydroxy-linalool	C10H18O2	170.1301	171.1380	153.1274	135.1169	hydroxy-dihydro-linalool	C10H20O2	172.1461		155.1431	137.1326
1,2- or 6,7- epoxy-linalool						1,2- or 6,7-epoxy-dihydro-linalool					
linalool oxide						Additional substructure detected					
8-oxo-dihydro-linalool							C7H10	94.0777	95.0859		
+ malonyl hexose (+C9H16O10 - 2H2O)	C19H30O10	418.1833	419.1911	401.1805							

Compound 13 - RT: 10.25 min			Detected masses		
Possible structure	Brut formula	Mass	[M+H] ⁺	[M+H-H ₂ O] ⁺	[M+H-2H ₂ O] ⁺
hydroxy-linalool	C10H18O2	170.1301	171.1379	153.1273	
1,2- or 6,7- epoxy-linalool					
linalool oxide					
8-oxo-dihydro-linalool					

Supplemental Figure 7: Linalool derivatives detected in UHPLC-Orbitrap analysis.

Top lists expected masses of reference compounds, dehydrated forms and derived fragments in ESI+ mode. Bottom lists detected masses of 13 linalool derivatives found in *Arabidopsis* flower methanol extracts and respective putative identification.



Supplemental Figure 8: GC-MS mass spectra of the linalool conversion products and references. Compounds were identified by comparison with authentic references (shown on figure) or by NMR.

Genotyping of *Arabidopsis* null mutant lines

PCR with T-DNA Left Border		
Insertion line	primer 1	primer 2
<i>TPS10</i> line 1	GCGTGGACCGCTTGCTGCAACT (LBb1)	CGTTGTCCGCAAAAAACGTTTCTTAATTG
<i>TPS10</i> line 2	GCGTGGACCGCTTGCTGCAACT (LBb1)	CGATCACAATATTGTGCTACAAGTG
<i>TPS14</i> line 1	GCGTGGACCGCTTGCTGCAACT (LBb1)	GATGTGGAGAAGGCAAGAAGCCAGCCG
<i>TPS14</i> line 2	GCGTGGACCGCTTGCTGCAACT (LBb1)	CCATTCTGGATCTTCTTGACCCGCG
<i>TPS14</i> line 3	GCGTGGACCGCTTGCTGCAACT (LBb1)	GGTTCTTCACGTTCTTCGGATTTGCTTCC
<i>CYP76C3</i> line 1	GCGTGGACCGCTTGCTGCAACT (LBb1)	AGAGCCATCGAGATTCCCGGAC
<i>CYP76C3</i> line 2	GCGTGGACCGCTTGCTGCAACT (LBb1)	AGAGCCATCGAGATTCCCGGAC
<i>CYP71B31</i> line 1	GCGTGGACCGCTTGCTGCAACT (LBb1)	CTTCCTTGTGAAGTGGTTTGC
<i>CYP71B31</i> line 2	GCGTGGACCGCTTGCTGCAACT (LBb1)	GATGTGCCTCGACAGAGTTGCC

PCR over insertion locus		
Insertion line	primer 1	primer 2
<i>TPS10</i> line 1	CGTGATCCCATTCCCTCAAAAAATC	CGTTGTCCGCAAAAAACGTTTCTTAATTG
<i>TPS10</i> line 2	GAGTTCCTCTTGATGAATAGCTTGTACG	CGATCACAATATTGTGCTACAAGTG
<i>TPS14</i> line 1	CGAACTCTGGCGAATGGCGTGG	GATGTGGAGAAGGCAAGAAGCCAGCCG
<i>TPS14</i> line 2	GGTCTTCACGTTCTTCGGATTTGCTTCC	CCATTCTGGATCTTCTTGACCCGCG
<i>TPS14</i> line 3	CCATTCTGGATCTTCTTGACCCGCG	GGTCTTCACGTTCTTCGGATTTGCTTCC
<i>CYP76C3</i> line 1	TGAAGCTTGGAAAGGTTAACCCG	AGAGCCATCGAGATTCCCGGAC
<i>CYP76C3</i> line 2	TGAAGCTTGGAAAGGTTAACCCG	AGAGCCATCGAGATTCCCGGAC
<i>CYP71B31</i> line 1	CACTGACTTCTCCCCAGAGG	CTTCCTTGTGAAGTGGTTTGC
<i>CYP71B31</i> line 2	CGACCGGCTCCAAAGGGCAAG	GATGTGCCTCGACAGAGTTGCC

Amplification of candidate genes

	Forward primer	Reverse primer
<i>TPS10</i>	GGCTTAAUATGGCCACTCTCTGCAA	GGTTTAAUTCAATCTAAAGGAATCGGATTG
<i>TPS10</i> without plastid transit sequence	GGCTTAAUATGCAGCGTCGTTCTGCG	GGTTTAAUTCAATCTAAAGGAATCGGATTG
<i>TPS14</i>	GGCTTAAUATGGCCTTAATAGCTACC	GGTTTAAUTTACATTAGAGACTTGAGATATTCCG
<i>TPS14</i> without plastid transit sequence	GGCTTAAUATGATCGATGTCATTCAAAGT	GGTTTAAUTTACATTAGAGACTTGAGATATTCCG
<i>CYP76C3</i>	GGCTTAAUATGGACCTCTCACTAATTCAAGG	GGTTTAAUTTAATAAGAAGACGATATTGTAGGTTTC
<i>CYP71B31</i>	GGCTTAAUATGTCTATGTTCTAGGTTTGCTC	GGTTTAAUTTATGGAAGAGTTGGTACGAGC

Amplification of promoter of candidate genes

	Forward primer	Reverse primer
Prom. <i>TPS10</i>	GGCTTAAUAGTTCTCGTGTGATTTGATGATAC	GGTTTAAUATTGAATAAATGTATTATTATGCTATACGTAAC
Prom. <i>TPS14</i>	GGCTTAAUCACCATTCGATTCAATTTTAAG	GGTTTAAUGATGTATGAACTTAAGTTTTGTTTTG
Prom. <i>CYP76C3</i>	GGCTTAAUCTGACTCTTATTGTGGTTTTTGT	GGTTTAAUTGGACGACCACTTTTTCTTTAGG
Prom. <i>CYP71B31</i>	GGCTTAAUCAATGATATGGACGATGACAG	GGTTTAAUGCAAACCTAGGAATATAGATATAATTATTG

Amplification of candidate genes and fusion with eGFP or mRFP

	Forward primer	Reverse primer
<i>TPS10</i>	GGCTTAAUATGGCCACTCTCTGCAA	ATGTGGCGACCGGUACCATCTAAAGGAATCGGATTG
<i>TPS14</i>	GGCTTAAUATGGCCTTAATAGCTACC	ATGTGGCGACCGGUACCCATTAGAGACTTGAGATATTCCG
<i>CYP76C3</i>	GGCTTAAUATGGACCTCTCACTAATTCAAGG	ATGTGGCGACCGGUACCATAAGAAGACGATATTGTAGG
<i>CYP71B31</i>	GGCTTAAUATGTCTATGTTCTAGGTTTGCTC	ATGTGGCGACCGGUACCTGGAAGAGTTGGTACGAGC
<i>eGFP</i>	ACCGGTCGCCACAUGGTGAGCAAGGGCGAGG	GGTTTAAUTTAGGCCATGATATAGACGTTGTGG
<i>mRFP</i>	ACCGGTCGCCACAUGGCCTCCTCCGAGGACGTCATC	GGTTTAAUTTAGGCGCCGGTGGAGTGGCG

qRT-PCR and RT-PCR

	Forward primer	Reverse primer
<i>TPS10</i>	ATCGTACAAGCTATTCATCAAGAGGAACT	ACCTAAACCTGTCTCCATCCACC
<i>TPS14</i>	GTCATTGACTCAAGGAGAAATGTCTCAAAC	GCTTCTTGCCCTTCTCCACATCTTT
<i>CYP76C3</i>	CCCGGAAACATTGACATGAGCGA	ACGATATTGTAGGTTTCTTGACGGGT
<i>CYP71B31</i>	CTTACGATCATCTCATAGCAATGATGTCGG	ATTGTTACTGTTCCAGCGTTTACTCCC
<i>SAND</i> (At2g28390)	GGATTTTCAGTACTCTTCAAGCTA	CTGCCTTGACTAAGTTGACACG
<i>TIP41</i> (At4g34270)	GAAGTGGCTGACAATGGAGTG	ATCAACTCTCAGCCAAAATCG
<i>PP2A</i> (At1g13320)	GACCGAGCCAACTAGGAC	AAAACCTGGTAACTTTTCCAGCA
<i>EXP</i> (At4g26410)	GAGCTGAAGTGGCTTCCATGA	GGTCCGACATACCCATGATCC

Supplemental Table 1: Primers used for genotyping of insertion lines, for amplification of ORFs and 1.5 kb-promoter region of candidate genes, and for qRT-PCR or RT-PCR.

***Arabidopsis* insertion mutant lines**

	SALK line name	Status
<i>tps10</i> line 1	SALK_108420	Homozygous
<i>tps10</i> line 2	SALK_041114	Homozygous
<i>TPS14</i> line 1	SALK_039462	Heterozygous
<i>TPS14</i> line 2	SALK_114189	Heterozygous
<i>tps14</i> line 3	SALK_059820	Homozygous
<i>cyp76c3</i> line 1	SALK_056876	Homozygous
<i>cyp76c3</i> line 2	SALK_077330	Homozygous
<i>cyp71b31</i> line 1	SALK_034144	Homozygous
<i>cyp71b31</i> line 2	SALK_009366	Homozygous
<i>tps10 tps14</i>	Selected after cross fecundation of <i>tps10</i> line 2 and <i>tps14</i> line 3	Homozygous

Supplemental Table 2: Name and status of employed *Arabidopsis* insertion mutant lines.

Gene Coexpression Analysis Reveals Complex Metabolism of the Monoterpene Alcohol Linalool in *Arabidopsis* Flowers

Jean-François Ginglinger, Benoit Boachon, René Höfer, Christian Paetz, Tobias G. Köllner, Laurence Miesch, Raphael Lugan, Raymonde Baltenweck, Jérôme Mutterer, Pascaline Ullmann, Franziska Beran, Patricia Claudel, Francel Verstappen, Marc J.C. Fischer, Francis Karst, Harro Bouwmeester, Michel Miesch, Bernd Schneider, Jonathan Gershenzon, Jürgen Ehlting and Danièle Werck-Reichhart

Plant Cell; originally published online November 27, 2013;
DOI 10.1105/tpc.113.117382

This information is current as of December 3, 2013

Supplemental Data	http://www.plantcell.org/content/suppl/2013/11/05/tpc.113.117382.DC1.html
Permissions	https://www.copyright.com/ccc/openurl.do?sid=pd_hw1532298X&issn=1532298X&WT.mc_id=pd_hw1532298X
eTOCs	Sign up for eTOCs at: http://www.plantcell.org/cgi/alerts/ctmain
CiteTrack Alerts	Sign up for CiteTrack Alerts at: http://www.plantcell.org/cgi/alerts/ctmain
Subscription Information	Subscription Information for <i>The Plant Cell</i> and <i>Plant Physiology</i> is available at: http://www.aspb.org/publications/subscriptions.cfm